

This document is confidential and is proprietary to the American Chemical Society and its authors. Do not copy or disclose without written permission. If you have received this item in error, notify the sender and delete all copies.

Discovery of Sisunatovir (RV521), an Inhibitor of RSV Fusion.

Journal:	<i>Journal of Medicinal Chemistry</i>
Manuscript ID	jm-2020-01882r.R2
Manuscript Type:	Drug Annotation
Date Submitted by the Author:	n/a
Complete List of Authors:	Cockerill, George; ReViral Ltd, R and D Angell, Richard; University College London School of Pharmacy Bedernjak, Alexandre; Reviral Ltd Fraser, Ian; CRL Chuckowree, Irina; University of Sussex Gascon, Jose; University of Sussex Gilman, Morgan; Harvard Medical School, Department of Biological Chemistry and Molecular Pharmacology Good, James; Reviral Ltd Harland, Rachel; ReviralLtd Johnson, Sarah; University of Michigan Medical School Littler, Edward; Reviral Ltd Ludes-Meyers, John; The University of Texas at Austin Lumley, James; GlaxoSmithKline Research and Development, Molecular Design, Data and Computational Sciences Lunn, Graham; University of Sussex Mathews, Neil; ReViral Ltd McLellan, Jason; The University of Texas at Austin, Molecular Biosciences Paradowski, Michael; Cardiff University, BIOSI Peeples, Mark; The Ohio State University College of Medicine Scott, Claire; Covance Tait, Dereck; Reviral Ltd Taylor, Geraldine; Pirbright Institute Thom, Michelle; Pirbright Institute Thomas, Elaine; Reviral Ltd Villalonga Barber, Carol; University of Sussex Ward, Simon; Cardiff University, Medicines Discovery Institute Watterson, Daniel; Univ Queensland Williams, Gareth; University of Sussex Young, Paul; The University of Queensland, School of Chemistry & Molecular Biosciences Powell, Kenneth; Reviral Ltd

SCHOLARONE™
Manuscripts

GRAPHICAL ABSTRACT

Discovery of Sisunatovir (RV521), an Inhibitor of RSV Fusion.

*G. Stuart Cockerill^{*a}, Richard M. Angell^{bt}, Alexandre Bedernjak^a, Irina Chuckowree^b, Ian Fraser^{a††}, Jose Gascon^b, Morgan S. A. Gilman^g, James A. D. Good^a, Rachel Harland^a, Sara M. Johnson^{e‡‡}, John Ludes-Meyers^g, Edward Littler^a, James Lumley^{a‡}, Graham Lunn^b, Neil Mathews^a, Jason S McLellan^g, Michael Paradowski^c, Mark E. Peeples^e, Claire Scott^{a#}, Dereck Tait^a, Geraldine Taylor^f, Michelle Thom^f, Elaine Thomas^a, Carol Villalonga Barber^b, Simon E. Ward^c, Daniel Watterson^d, Gareth Williams^b, Paul Young^d, Kenneth Powell^a.*

^aReViral Ltd., Stevenage Bioscience Catalyst, Gunnels Wood Road, Stevenage, Hertfordshire. SG1 2FX. UK. ^bSussex Drug Discovery Centre, University of Sussex, Brighton, England BN1 9QJ, UK. ^cMedicines Discovery Institute, Cardiff University, Cardiff, Wales, CF10 3AT, UK ^dSchool of Chemistry and Molecular Biosciences, The University of Queensland, Brisbane, Queensland 4072, Australia. ^eCenter for Vaccines and Immunity, The Research Institute at Nationwide Children's Hospital, and Department of Pediatrics, The Ohio State University College of Medicine,

1
2
3 Columbus, Ohio 43205, USA. ^fThe Pirbright Institute, Ash Road,
4
5 Pirbright, Surrey, GU24 0NF, UK. ^gDepartment of Molecular
6
7 Biosciences, The University of Texas at Austin, Austin, TX 78712,
8
9 USA.
10
11
12
13
14
15
16
17
18
19
20
21
22
23
24
25
26
27
28
29
30
31
32
33
34
35
36
37
38
39
40
41
42
43
44
45
46
47
48
49
50
51
52
53
54
55
56
57
58
59
60

Discovery of Sisunatovir (RV521), an Inhibitor of Respiratory Syncytial Virus Fusion.

*G. Stuart Cockerill^{*a}, Richard M. Angell^{bt}, Alexandre Bedernjak^a, Irina Chuckowree^b, Ian Fraser^{a††}, Jose Gascon^b, Morgan S. A. Gilman^g, James A. D. Good^a, Rachel Harland^a, Sara M. Johnson^{e‡‡}, John Ludes-Meyers^g, Edward Littler^a, James Lumley^{a‡}, Graham Lunn^b, Neil Mathews^a, Jason S McLellan^g, Michael Paradowski^c, Mark E. Peeples^e, Claire Scott^{a#}, Dereck Tait,^a Geraldine Taylor^f, Michelle Thom^f, Elaine Thomas^a, Carol Villalonga Barber^b, Simon E. Ward^c, Daniel Watterson^d, Gareth Williams^b, Paul Young^d, Kenneth Powell^a.*

^aReViral Ltd., Stevenage Bioscience Catalyst, Gunnels Wood Road, Stevenage, Hertfordshire. SG1 2FX. UK. ^bSussex Drug Discovery Centre, University of Sussex, Brighton, England BN1 9QJ, UK. ^cMedicines Discovery Institute, Cardiff University, Cardiff, Wales, CF10 3AT, UK ^dSchool of Chemistry and Molecular Biosciences, The University of Queensland, Brisbane, Queensland 4072, Australia. ^eCenter for Vaccines and Immunity, The Research Institute at Nationwide Children's Hospital, and Department of

1
2
3 Pediatrics, The Ohio State University College of Medicine,
4 Columbus, Ohio 43205, USA. ^fThe Pirbright Institute, Ash Road,
5
6 Pirbright, Surrey, GU24 0NF, UK. ^gDepartment of Molecular
7
8 Biosciences, The University of Texas at Austin, Austin, TX 78712,
9
10
11
12 USA.

13
14
15
16
17
18
19 KEYWORDS Drug Discovery, Orally Bioavailable. Respiratory
20
21 Syncytial Virus. Fusion Inhibitor.

22
23 ABSTRACT: RV521 is an orally bioavailable inhibitor of
24
25 Respiratory Syncytial Virus (RSV) fusion that was identified after
26
27 a lead optimization process based upon hits that originated from
28
29 a physical property directed hit profiling exercise at Reviral.
30
31 This exercise encompassed collaborations with a number of contract
32
33 organizations, with collaborative medicinal chemistry and virology
34
35 during the optimization phase in addition to those utilized as the
36
37 compound proceeded through pre-clinical and clinical evaluation.
38
39 RV521 exhibited a mean IC₅₀ of 1.2 nM against a panel of RSV A and
40
41 B laboratory strains and clinical isolates with antiviral efficacy
42
43 in the Balb/C mouse model of RSV infection. Oral bioavailability
44
45 in preclinical species ranged from 42% to >100%, with evidence of
46
47 highly efficient penetration into lung tissue. In healthy adult
48
49 human volunteers experimentally infected with RSV, a potent
50
51
52
53
54
55
56
57
58
59
60

1
2
3 antiviral effect was observed with a significant reduction in viral
4
5 load and symptoms compared to placebo.
6
7

8 9 INTRODUCTION

10
11
12
13 Respiratory syncytial virus (RSV) is an RNA virus of the
14 *Pneumoviridae* family and is responsible for a seasonal and global
15
16 respiratory tract infection. Patient populations most at risk of
17
18 severe disease from RSV are specifically patients with weakened
19
20 immune function due to old age or immature immune and physical
21
22 development¹. Populations at risk are premature infants,
23
24 immunocompromised adults, COPD (chronic obstructive pulmonary
25
26 disease), CHF (chronic heart failure) patients and the elderly.
27
28 The viral infection can progress to lower respiratory tract
29
30 infection (LRTI) and result in airway inflammation, bronchiolitis,
31
32 pneumonia and in extreme cases, respiratory failure. Premature
33
34 infants and young children with underlying heart disease or
35
36 pulmonary dysplasia have the highest risk of severe disease
37
38 resulting from RSV LRTI.² RSV is associated with significantly
39
40 more deaths and infant hospitalizations than influenza,³
41
42 parainfluenza, or human metapneumovirus. Additionally severe RSV
43
44 infection in infancy is linked to the later development of asthma.⁴
45
46
47
48
49
50

51
52 Despite the clear impact of the virus and associated economic
53
54 burden, limited treatments exist for RSV disease. No vaccine exists
55
56
57
58
59
60

1
2
3 and only palivizumab,⁵ a monoclonal antibody (mAb), approved for
4 prophylaxis and ribavirin, a broad-spectrum nucleoside antiviral
5 drug of low efficacy have been approved. The standard of care for
6 RSV-infected patients remains supportive, including fluids and
7 oxygen.⁶
8
9

10 RSV contains a single stranded linear RNA genome with 10 genes
11 encoding 11 proteins.^{7, 8} Proteins of interest to drug discovery
12 programs have been the L (RNA polymerase), the N (nucleoprotein),
13 M (Matrix protein), M2.1 and the F (fusion protein). This paper
14 describes our approach to inhibitors of the fusion protein, given
15 its fundamental importance in viral infectivity and also its
16 conserved nature.
17
18
19
20
21
22
23
24
25
26
27
28
29
30

31 32 RESULTS AND DISCUSSION

33 A perspective on the position of anti-RSV drug discovery in 2018
34 described the progression of several direct acting antivirals for
35 the treatment of RSV into clinical trials, targeting both fusion
36 and replication.⁹ When this particular project was initiated in
37 2011, the field was far less mature, indeed only RSV604, an RSV
38 nucleocapsid protein inhibitor had demonstrated efficacy, and that
39 in a subanalysis of stem cell transplant patient data¹⁰. Recently
40 data has been disclosed for both presatovir¹¹ **1** and JNJ-53718678¹²
41 **2** in adult and pediatric patient populations respectively.
42 Additionally, an inhibitor of RSV fusion, ziresovir¹³ **3** and EDP-
43
44
45
46
47
48
49
50
51
52
53
54
55
56
57
58
59
60

938,¹⁴ an N protein inhibitor (structure not disclosed), have progressed into the human challenge model and phase 2 trials (Figure 1).

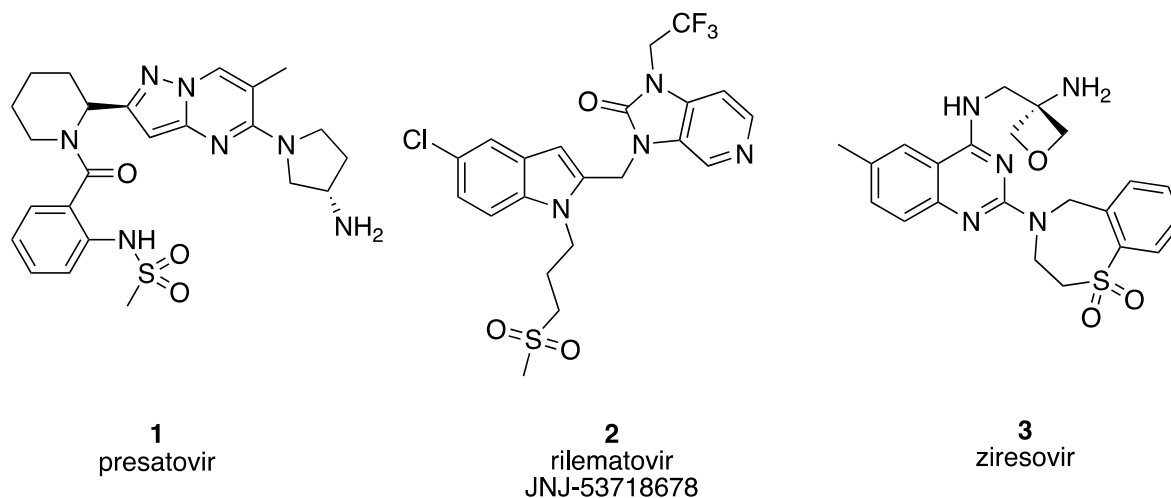


Figure 1. Clinical stage RSV fusion inhibitors.

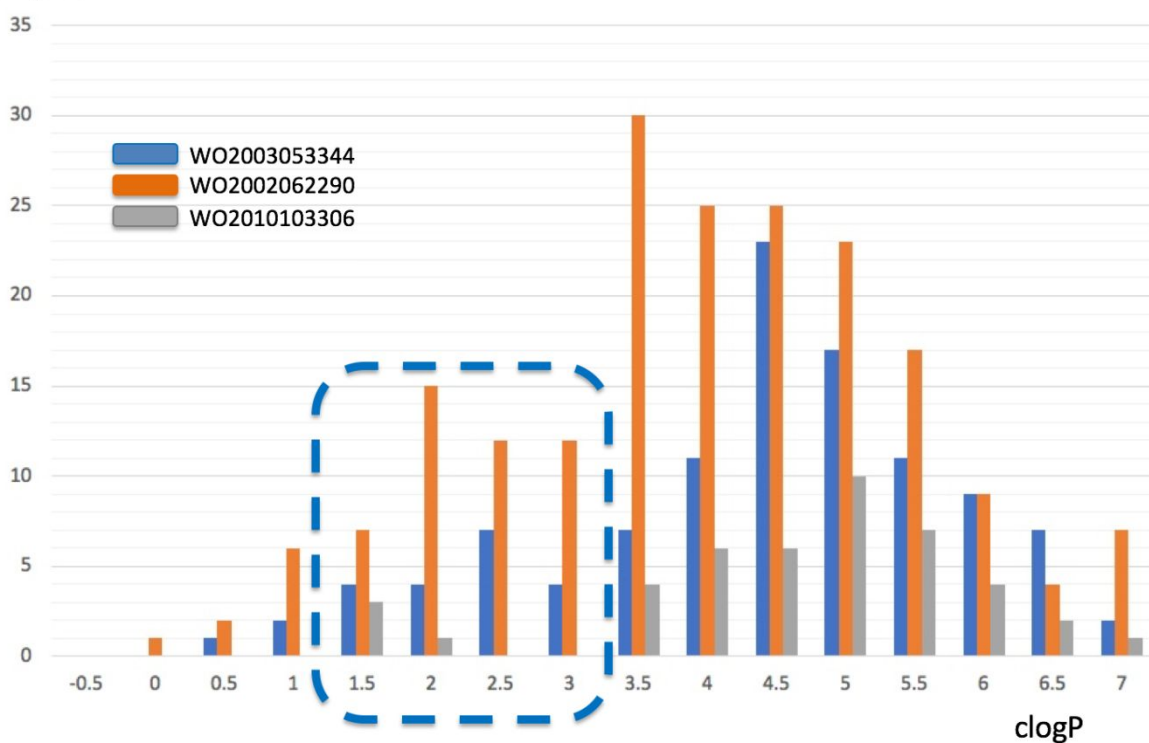
Hit Identification.

We focused our attention on the fusion target, not least because in addition to its key role in the infectivity process, there were small molecule fusion templates that possessed inherent developability advantages, specifically in terms of molecular size, physical properties and potency that could lead to a hit compound worthy of progression. We focused our attention on a cyclic urea/benzimidazole scaffold previously described.¹⁵ This series looked to have beneficial optimization properties over other fusion archetypes known at that time. Although it was unclear why compounds had failed to progress in 2011, subsequent

1
2
3 summaries have appeared.¹⁶ As part of our analysis, we looked at
4 the physical properties of compounds prepared in this series from
5 a number of sources. A typical output is shown in **Figure 2**. We
6 examined a number of patents pertaining to RSV fusion inhibitors¹⁷
7 -¹⁹ and identified a clear trend toward higher clogP values, with
8 the majority of compounds possessing values greater than 3.5. The
9 detrimental effects of higher clogP values have been documented.
10
11
12
13
14
15
16
17
18
19
20
21
22
23
24
25
26
27
28
29
30
31
32
33
34
35
36
37
38
39
40
41
42
43
44
45
46
47
48
49
50
51
52
53
54
55
56
57
58
59
60

Our intention was to focus our modifications to restrict our clogP figure to less than 3.5 to enhance the development potential of any candidate clinical compound.

Examples



1
2
3 **Figure 2.** A plot of numbers of compounds disclosed in three
4 benzimidazole patents against clogP.¹⁶⁻¹⁸ clogP figures represent
5 the central point of each bin covering clogP values +/- 0.25. ClogP
6 values were calculated using Biobyte version 5.4
7 (<http://www.biobyte.com/index.html>). Patent example data was
8 extracted from Surechembl (<https://www.surechembl.org/search/>).
9 Examples with MWt outside of the range 300-700 were removed and
10 structures were checked manually with reactive compounds removed.
11
12
13
14
15
16
17
18
19
20
21
22
23

24 In what was an increasingly complex patent space,⁹ structural
25 novelty was a key consideration. Despite this complexity, we had
26 analyzed the patent space associated with the area and identified
27 spirocyclic systems as possessing the required novelty. We
28 therefore focused our initial synthetic program on a novel range
29 of spirocyclic ring containing heterocycles, by constructing
30 spirocyclic systems anchored to a bicyclic oxindole or the
31 corresponding tetrahydroquinolinone component of the fusion
32 inhibitor (**Figure 3**).
33
34
35
36
37
38
39
40
41
42
43
44
45
46
47
48
49
50
51
52
53
54
55
56
57
58
59
60

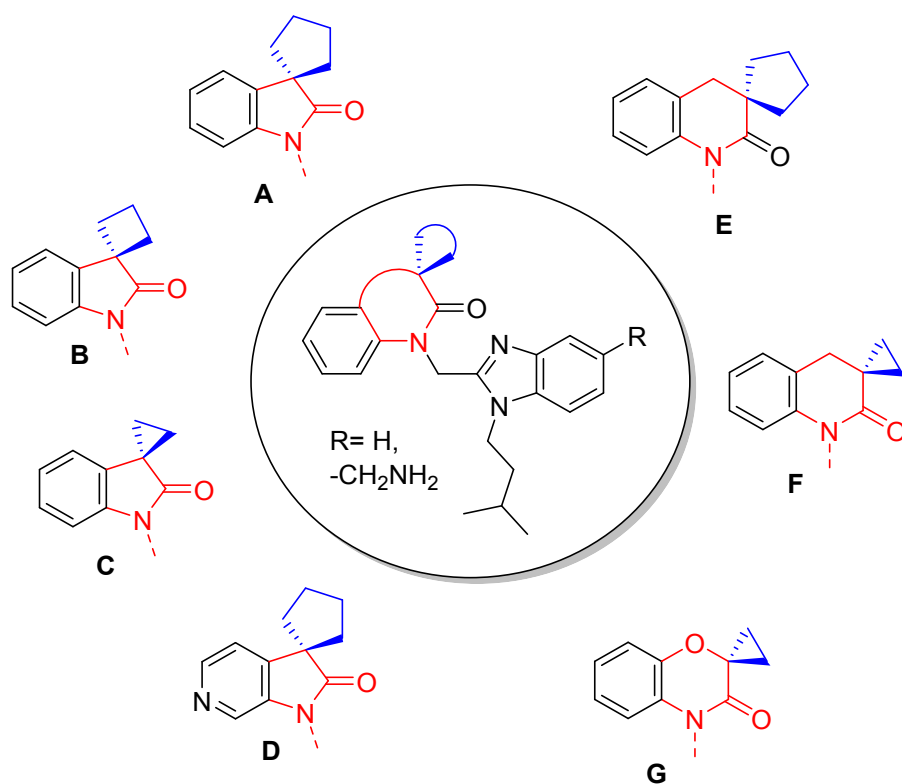
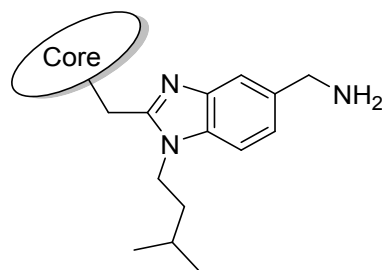


Figure 3. Summary of spirocyclic structural scan, with cores **A-G** used in the initial hit finding exercise. The five and six membered lactam cores are shown in red and the proposed three to five membered spirocycles in blue.



Cmpd	Core	RSV A2 PRA EC ₅₀ (nM)	CC ₅₀ (μM)	cLogD _{7.4}
4	A	580	9.94	2.84
5	B	240	13.75	2.39

6	C	31	15.29	1.95
7	D	310	23.11	1.62
8	E	14,000	11.54	3.28
9	F	3,400	33.4	2.39
10	G	1,700	22.7	1.69

Table 1. Spirocyclic compounds prepared during the hit finding exercise. Cores and R group as defined in **Figure 3**. The plaque reduction assay (PRA) was performed in Vero cells with the RSV A2 strain. CC₅₀ refers to Vero cell cytotoxicity and was assessed by MTT staining. EC₅₀ and CC₅₀ values are an average of at least 2 testing occasions. clogD_{7.4} were calculated using Marvin software 18.16.0, 2018, ChemAxon (<http://www.chemaxon.com>.)

This limited structural scan, of three to five membered ring containing spiro systems, allowed the observation of a structure activity pattern, which was most apparent with an amino methylene benzimidazole scaffold (**Figure 3** and **Table 1**). Potency against the virus was measured using an RSV A2 strain plaque reduction assay (PRA) in Vero cells with cellular cytotoxicity measured in parallel. Significant potency was observed with a 6,5 oxindole containing a spirocyclopropyl (compound **6**), whilst oxindoles containing larger spirocyclic ring systems (**4**, **5** and **7**) were less potent in this smaller oxindole system. The larger 6,6 systems, either tetrahydroquinolinone or tetrahydropyranone **8-10** were observed to be markedly less potent (**Table 1**). A comparative study

with unsubstituted benzimidazole series demonstrated analogous trends but with poorer activities generally (data not shown); in this less active series the corresponding spirocyclobutyl oxindole was the most potent analogue ($EC_{50} >7.5\mu\text{M}$). We were encouraged that the structure activity trends were in line with our physicochemical targets; clogP and clogD values were acceptable at this stage, particularly for the smaller ring sizes.

Table 2a.

Cmpd	Kinetic solubility ^a (μM)	$P_{\text{app}}^{\text{b}}$ ($10^{-6} \text{ cm s}^{-1}$)	PPB F_u (%) rat, dog, human	Microsomal CL_{int} ($\mu\text{L}/\text{min}/\mu\text{g}$ protein) rat, dog, human.	Microsomal $t_{1/2}$ (min) rat, dog, human
6	155	12	10, 10, 7	<19, <28, 592	>95, >100, 5
7	160	11	24, 14, 17	<31, <28, 488	>89, >100, 6

Table 2b.

Mouse Pharmacokinetics for compound 6 ^c				
Cmpd	C_{max} (oral) (ng/mL)	Clearance (i.v.) (mL/min/kg)	Vd_{ss} (i.v.) (L/kg)	F%
6	6	98	34	4

Table 2a and **2b.** *in vitro* (**2a**) and *in vivo* (**2b**) pharmacokinetic data for leading compounds from the hit finding exercise. ^a

Kinetic solubility determined by the addition of the compound in DMSO to 0.1 M PBS at pH 7.4; precipitation of the compound was measured at a range of concentrations. ^b Apparent permeability (P_{app}) in a wild type unidirectional MDCK cell assay. ^c The

1
2
3 compound was dosed as a suspension of the amorphous solid at 1
4
5 mg/kg iv and 5 mg/kg po.
6
7

8 Profiling of leading compounds **6** and **7** from this exercise in an
9
10 *in vitro* ADME and physicochemical screen showed compounds with
11
12 good solubility, permeability and plasma protein binding unbound
13
14 fractions (**Table 2a**). Clearance data was acceptable in rodent
15
16 and dog microsomes although half-lives were low in human
17
18 microsomes. We progressed the most potent compound **6** into a mouse
19
20 *in vivo* pharmacokinetic study. We observed a low level of exposure
21
22 (F, 4%, C_{max} 6 ng/mL) with high clearance (98 mL/min/kg). In light
23
24 of this high clearance, we employed a microsomal ID study in rat
25
26 and human microsomes to investigate the metabolic susceptibility
27
28 of the molecule. In this study, the lead compound **6** was incubated
29
30 at 10 μM with microsomes isolated from liver hepatocytes and sites
31
32 of metabolism were subsequently proposed from mass spectral
33
34 analysis of fragmentation patterns (**Error! Reference source not**
35
36 **found.**). Significantly, greater turnover was observed in
37
38 incubations with human microsomes than the rat system. This
39
40 correlated with the previously observed microsomal clearance data
41
42 (**Table 2a**). Most interestingly, both human specific metabolites
43
44 and those observed in both species were confined structurally to
45
46 the cyclopropyl oxindole fragment of the molecule.²² Although
47
48 hydroxylation metabolites were proposed in the rat microsomal
49
50
51
52
53
54
55
56
57
58
59
60

1
2
3 incubation, a specific mono-hydroxylation metabolite was far more
4 prevalent in human microsomes, double hydroxylation metabolites
5 were only observed in the human incubation (see supplementary
6 information). This focused our attention on the cyclopropyl
7 oxindole.
8
9
10
11
12
13

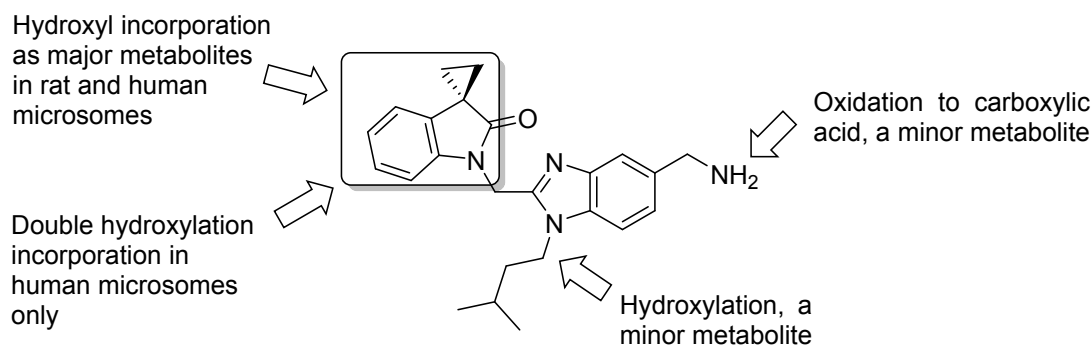


Figure 4. Summary of metabolite ID study for compound 6 following incubation with microsomes derived from rat and human liver cells. Most likely sites of metabolism are indicated by arrows.

This point in time represented a key moment for the project and ReViral; we had identified a potent hit compound, with pharmacokinetic properties that demonstrated some level of oral bioavailability, albeit with the aforementioned metabolic liability (**Tables 2a** and **2b**). This series of compounds we believed possessed potential for good oral absorption properties.²² Additionally, a high volume of distribution was observed in this compound *in vivo*. The link between compound distribution and

1
2
3 clearance could not be ignored. Indeed, a positively distributing
4
5 compound would be expected to attain higher concentrations in
6
7 target tissue than those observed in the plasma compartment²³, with
8
9 a potential beneficial effect for efficacy studies. The
10
11 metabolite study itself provided us with a clear plan and the
12
13 potential for a productive optimization process. Initial studies
14
15 in the next phase of the project were directed towards blocking
16
17 metabolism on the oxindole.
18
19
20
21

22 **Lead Optimization.**

23
24
25 The project employed a design, make and test framework whereby
26
27 compounds were tested initially in an RSV fusion reporter-based
28
29 cell-cell fusion assay (in human embryonic kidney 293T cells)
30
31 before subsequent antiviral evaluation in the whole virus RSV A2
32
33 plaque assay (**Figure 5**). This fusion assay²⁴ was a higher
34
35 throughput assay that allowed an efficient generation of initial
36
37 activity data and was importantly for us co-located with the
38
39 medicinal chemistry group. We progressed compounds with fusion
40
41 $IC_{50} \leq 5$ nM into the plaque assay which was run at distance by a
42
43 collaborator. Compounds were then evaluated in physicochemical
44
45 and pharmacokinetic assays on contract. Some changes took place
46
47 at this point, specifically the contractor supplying *in vitro*
48
49 ADME/physical property determination assays. At a later stage in
50
51 the project, the development of a company "in house" antiviral
52
53
54
55
56
57
58
59
60

capability led to the use of additional cell lines. For example, HepG2 cells and Hep2 cells were added in the cell toxicity screen. Where this affects data in this paper the alternate cell lines used are indicated. Despite these changes, toxicity data for compounds retained a consistent profile in these assays.

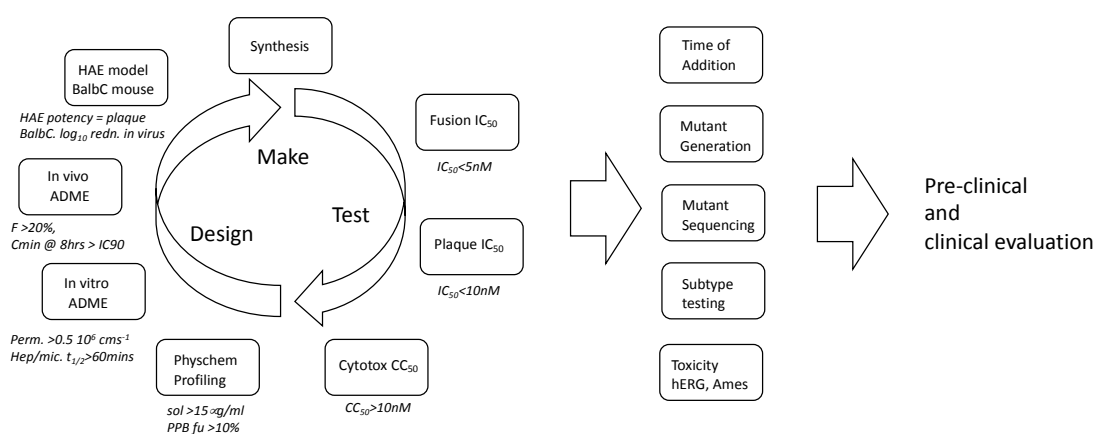


Figure 5. Project flowchart depicting the design, make and test cycle for compounds prepared in the project. The design, make, test cycle allowed a progression to *in vivo* evaluation in the mouse BalbC model. Detailed virology and toxicity analysis prior to progression into pre-clinical evaluation followed. Generalized progression criteria are shown in italics below or alongside each assay.

1
2
3 Compounds satisfying our basic criteria for progression would
4
5 progress into two key antiviral assays: the human airway epithelial
6
7 (HAE) model,²⁵ whereby differentiated human epithelial cell
8
9 cultures were infected with a luciferase expressing RSV, and the
10
11 use of the Balb/C mouse RSV infection model to study *in vivo*
12
13 efficacy (*vide infra*).²⁶
14
15
16

17
18 Detailed analysis followed for a compound satisfying our potency
19
20 and pharmacokinetic requirements; principally this comprised
21
22 testing against a range of RSV A and B laboratory strains and low
23
24 passage clinical isolates of RSV A and B. Consistent activity
25
26 against these strains was an important requirement for any compound
27
28 to progress given that RSV A and B strains co-circulate during an
29
30 infectious season. Additionally, there was now a longer-term
31
32 commitment to perform experiments to raise and subsequently
33
34 sequence the RNA of resistant mutants to such a compound. The
35
36 complexity of these later-stage virology studies restricted them
37
38 to the analysis of a compound moving towards clinical evaluation
39
40 and were performed as an integral part of the company's in-house
41
42 capability as it evolved.
43
44
45
46
47
48
49
50
51
52
53
54
55
56
57
58
59
60

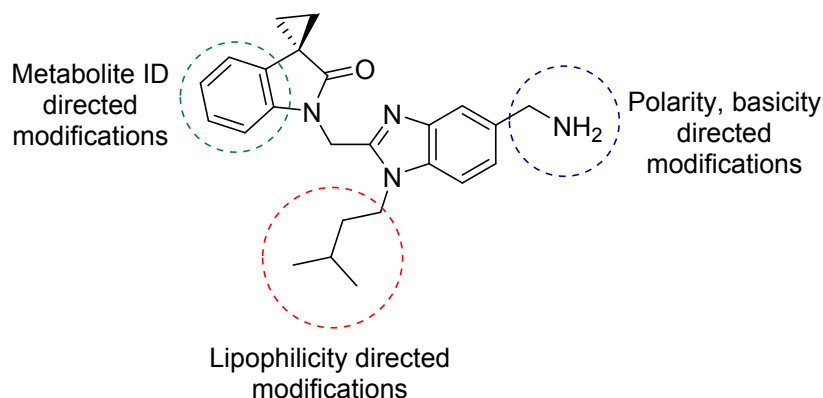


Figure 6. Structural modification strategies employed in the lead optimization of hit **6**.

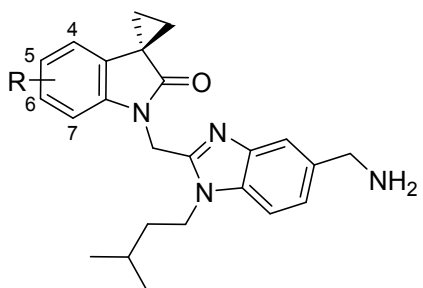
The medicinal chemistry strategy employed during this phase of the project was to target three key areas of the lead compound **6** depicted in **Figure 6**. An initial focus on introduction of substituents into the oxindole portion of the molecule to help block metabolism was followed by targeted modifications of the chain substituting the benzimidazole and modifications to the basic aminomethylene functionality. Approaches to analogues of the aza-oxindole **7** were of lower priority within the research team, due to the lower potency of this lead compound and practical issues associated with the synthesis of the spirocyclic aza-oxindole fragment at this stage in the project. Compounds subsequently derived from lead **7** are reviewed briefly at the end of this section (**Figure 7**).

Spirocyclopropyl oxindole ring modification

1
2
3 The initial LO studies were aimed at the introduction of
4 stabilizing groups into the oxindole portion of the lead compound
5 as directed by our earlier metabolite ID study. **Table 3** shows a
6 selection of substituents that were successfully introduced as
7 part of this exercise. The emphasis at this stage was focused on
8 small halogen substituents that would represent as small a physical
9 property change as possible whilst functioning in a metabolic
10 blocking role. Potency could be retained for 5- and 6- chlorine
11 substituted compounds (**13** and **15 Table 3**) relative to compound
12 (**6**), 4- and 7- chlorine substitution had a deleterious effect (**11**
13 and **16**), whereas 5- and 6-fluorine substitution produced the most
14 potent analogues (**12** and **14**); with the synthetically more
15 accessible 6-regioisomer **14** marginally more potent. Cell assay
16 variability has to be taken into account with this data and it was
17 seen that the fusion assay grouped analogues into tighter groups
18 of potent and less potent modifications. In the light of the later
19 crystal structure of RV521 bound to the trimeric pre-hairpin
20 binding pocket (PDB code 7KQD); the binding of the oxindole
21 component into a small well-defined pocket is evident (**Figure 9**,
22 particularly panel b). One would suspect a chlorine substituent
23 would explore the steric limitations of this pocket with direct
24 ligand protein steric effects and conformational effects upon the
25 ligand itself (particularly in the 7 position). 6-Fluoro
26
27
28
29
30
31
32
33
34
35
36
37
38
39
40
41
42
43
44
45
46
47
48
49
50
51
52
53
54
55
56
57
58
59
60

1
2
3 substitution direct ligand/protein interactions are harder to
4
5 discern but there could be beneficial binding effects.
6
7

8
9 The evaluation of compounds in *in vitro* ADME studies (**Table 4**)
10 provided new data for us at this stage. The permeability assay
11 was changed to a bi-directional assay in MDCK cells, as opposed to
12 the previously employed unidirectional system in the same cell
13 line. Additionally, the solubility assay method was changed to
14 assess thermodynamic solubility, amorphous solid compound was now
15 administered to aqueous buffer and solubility assessed over 24
16 hours as opposed to an administration of compound in DMSO to
17 buffer. The lead compounds **12** and **14** exhibited good solubility in
18 this assay and maintained reasonable protein binding unbound
19 fraction figures. They were profiled alongside the 7-fluorine
20 substituted regioisomer **17**. There was some variability observable
21 in unbound fraction between species for these compounds and
22 microsomal clearance was still significant but did seem to show an
23 improvement for compound **12** in human microsomes over compound (**6**).



Cmpd	Substituent R	RSV Fusion IC ₅₀ (nM)	RSV A2 Plaque EC ₅₀ (nM)	CC ₅₀ (nM)
6	H	0.4	31	15,290
11	4-Cl	11.1	180.7	5,200
12	5-F	0.7	4.2	7,600
13	5-Cl	4.5	25.4	710
14	6-F	0.5	0.8	3,000
15	6-Cl	1.2	6.7	4,500
16	7-Cl	46.7	2384.3	21,700
17	7-F	1.3	40.8	31,100

Table 3. Lead optimization of hit spirocycle (**6**): antiviral activity and cell toxicity for compounds prepared as a result of the metabolite ID study. The RSV cell fusion assay was performed in human embryonic kidney 293T cells co-transfected with RSV F protein from the RSV A2 strain or an expression plasmid encoding a transcriptional transactivator fusion protein. The plaque reduction assay (PRA) was performed in Vero cells with the RSV A2 strain. CC₅₀ refers to Vero cell cytotoxicity and was assessed by MTT staining. IC₅₀, EC₅₀ and CC₅₀ values are an average of at least 2 testing occasions.

The permeability of the 7-fluoro example **17** was low, and both of these regioisomeric compounds **14** and **17** exhibited significant efflux ratios. No advantage was observed with the 5-fluoro analogue **12** as this compound exhibited a very high clearance in human microsomes and a low to moderate permeability in the unidirectional permeability assay (CL_{int}: 344 μL/min/μg protein, t_{1/2} = 8 minutes; P_{app} = 7.3 10⁻⁶ cms⁻¹). When evaluated in *in vivo*

1
2
3 pharmacokinetic studies (**Table 4b**), the 6-fluoro compound **14** was
4
5 more promising with a bioavailability of 25% versus 8.8% for **17** in
6
7 rats (10 mg/kg oral, 1 mg/kg iv), however clearance remained high.
8
9 The disconnect observable between *in vitro* microsomal clearances
10
11 and the *in vivo* clearance for all these compounds has to be taken
12
13 in context with the large volumes of distribution observable for
14
15 these compounds (**6**, **14** and **17**, **Table 4b**). The consensus at this
16
17 point was that we were indeed in a position whereby we had modified
18
19 the metabolic lability of the compounds; however, the distributive
20
21 properties of the compounds clouded the overall picture. A high
22
23 volume of distribution, since it relates the total body
24
25 concentration of drug to the drugs plasma concentration, would
26
27 actually be reflected in enhanced clearance figures.^{23a} We
28
29 progressed the optimization of these compounds with the view that
30
31 retaining good distribution properties was a favorable
32
33 characteristic, indeed the presystemic extraction of drugs that
34
35 can be classed as lipophilic amines in organs such as the lung is
36
37 documented^{23b}. This strategy was borne out ultimately in the
38
39 properties of RV521 (**20**, *vide infra*). At this point we turned our
40
41 attention to chain modifications.
42
43
44
45
46
47
48
49

Table 4a

	Thermo. Solubility^a	P_{app}^b (10⁻⁶ cm s⁻¹) A₂B/B₂A; ER	PPB F_u (%) rat, dog, human	Microsomal CL_{int} (μL/min/μg protein)	Rat Liver Hepatocyte CL_{int}
--	---------------------------------------	--	--	--	--

	(μM)			rat, dog, human	($\mu\text{L}/\text{min}/10^6$ cells)
6	155	(12) ^c	10, 10, 7	<19, <28, 592	ND
12	ND	(7.3) ^c	19, 15, 11	<29, <29, 344	ND
14	176.3	0.75/65.6 ; 88	33.3, 15.1, 18.4	45, 6.23, 50.7	43.1
17	1,230	0.19/42.1 ; 227	10.4, 14.7, 42	37.8, 2.23, 7.0	ND

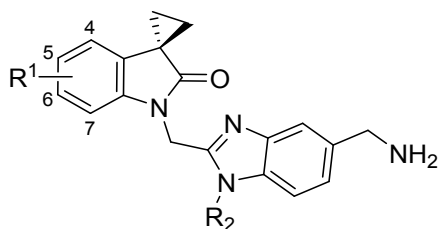
Table 4b

Cmpd	Rat Pharmacokinetic properties <i>in vivo</i> ^d			
	C _{max} (oral) (ng/mL)	Clearance (<i>iv</i>) (mL/min/kg)	Vd _{ss} (<i>iv</i>) (L/kg)	F%
6	6	98	34	4
14	44.2	174.0	54.3	25.0
17	31.3	107.7	11.9	8.8

Table 4. *in vitro* (Table 4a) and *in vivo* (Table 4b) pharmacokinetic data for leading compounds from lead optimization of the oxindole. ^a Thermodynamic solubility at pH 7.4 was determined by addition of aqueous solvent to solid compound and mixed overnight. The saturated solution was filtered and quantified against a DMSO stock solution using LC-UV. ^b Permeability assay in MDCK (MDR1) cells. Direction is indicated by A₂B or B₂A. ER denotes efflux ratio. ^c Permeability data from a wild type unidirectional MDCK cell assay. ^d Compounds were dosed as a suspension of the amorphous solid at 1 mg/kg *iv* and 5 mg/kg *po*.

Benzimidazole chain modifications

The benzimidazole chain substituent was a major lipophilic component of the structure, in addition there was some level of evidence for this chain as a target of metabolism (**Figure 4**). Our strategy was to reduce the lipophilicity of this chain substituent without a significant increase in polar surface area. This approach would allow us to reduce the overall lipophilicity with the benefit of improving solubility and the metabolic profile. We would hope to whilst retain the acceptable permeability observed thus far.



Cmpd	R ¹	R ²	RSV Fusion IC ₅₀ (nM)	RSV A2 Plaque EC ₅₀ (nM)	CC ₅₀ (nM)	ΔclogD _{7.4} ^a	PSA (Å ²)
18	6-F		2.6	5.7	>25,000	-2.87	98.3
19	6-F		1.5	3.6	>25,000	-1.23	84.4
20	6-F		0.9	1.3	5,588	-0.1 ^b	64.2
21	7-F		1.0	2.3	>25,000	-0.1	64.2
22	6-F		2.6	1.6	>25,000	-1.2	84.4
23	6-F		1.2	2.4	>25,000	-1.65	73.4

1
2
3 **Table 5.** Chain modification antiviral activity and calculated
4 physicochemical properties. The plaque reduction assay (PRA) was
5 performed in Huh-7 cells with the RSV A2 strain. IC₅₀ and EC₅₀
6 values are an average of at least 2 testing occasions. CC₅₀ refers
7 to cell cytotoxicity measured in HepG2 cells.. ^a ΔclogD_{7.4} values
8 are calculated by comparison with the parent iso-pentyl
9 substituent compounds **14** and **17** (clogD_{7.4} 2.09 for both compounds).
10 Values were calculated using Marvin. (Marvin 16.5.16.0, 2016,
11 ChemAxon (<http://www.chemaxon.com>)). ^b clogD_{7.4} for compound **20** is
12 2.00.
13
14
15
16
17
18
19
20
21
22
23
24
25
26
27
28

29 In general, as observed in other reported inhibitors of RSV F
30 protein,¹² chains with four to five atoms were acceptable in terms
31 of potency and most interestingly, cyclic systems, such as
32 cyclohexanol (**22**) or pyran (**23**) were also potent in the RSV plaque
33 and fusion assays (**Table 5**). In the case of the pharmacokinetics
34 of cyclohexanol **22** (**Tables 6 and 8**), low permeability and low
35 clearance was observed *in vitro* (P_{app} MDCK-MDR1A2B/B2A; ER 0.13/
36 2.8; 21 10⁻⁶ cm s⁻¹, 0.13 mL/min/mg protein in rat microsomes), and
37 high clearance and low bioavailability in mice (82.7 mL/min/kg, F
38 4.4%).
39
40
41
42
43
44
45
46
47
48
49
50

51 Low permeabilities were observed with the methylsulfonylpropyl
52 chain compound **18**, perhaps as a result of increased polar surface
53
54
55
56
57
58
59
60

area and lowered clogP. This low permeability was reflected in poor pharmacokinetics in the mouse, no oral exposure was seen for this compound (data not shown). The introduction of either the pyran or trifluorobutyl chain provided acceptable permeabilities in addition to reduced clogPs for the pyran (**23**) and a polar surface area figure below 70 Å² for the trifluorobutyl substituted systems (**20**) and (**21**). Conventionally viewed as a lipophilic substituent, the trifluorobutyl system can be viewed in a different perspective. A matched pair analysis reported by Böhm *et al* described the contextual dependence of the fluorine as a logP lowering or raising substituent. They described how the polarity increase of the fluorine atoms overcompensated for their lipophilic nature functioning as logP lowering substituents in their study.²⁷

Cmpd	Thermo. Sol. ^a (µM)	P _{app} ^b (10 ⁻⁶ cm s ⁻¹) A ₂ B/B ₂ A; ER	PPB ^c F _u (%) r/d/h	Microsomal ^c CL _{int} (µL/min/µg protein) r/d/h	Microsomal t _{1/2} (min) r/d/h	Hepatocyte ^c CL _{int} (µL/min/10 ⁶ cells) r/d/h	Hepatocyte t _{1/2} (min) r/d/h
18	2,595	0.24/0.79; 3.26	ND	3.63/5.34/3.78	ND	ND	ND
20	417	0.5/73; 146	52/27/67	17/2.6/44	80/532/32	14.8/2.4/6.58	93/580/211
21	1178	0.4/2.7; 7.5	ND	0.7/2.0/2.9	ND	ND	ND
22	313	0.1/2.8; 21	ND	9.4 / 5.02 / 4.6	147/276/300	ND	

23	1270	0.4/40.6 ; 94	39.9/4 9.7/54 .8	5.2/0.4/66 .4	246/3350 /20.9	21.2/0.8/7 .1	61.4/>100 0/197
33	ND	0/0.14: ND	ND	71.3/328/1 77	ND	ND	ND
35	ND	0/0.1:ND	ND	328.0 / 71.3 / 177.0	ND	ND	ND

Table 6. *in vitro* ADME data for selected examples prepared as part of the chain modification process. ^aThermodynamic solubility at pH 7.4 was determined by addition of aqueous solvent to solid amorphous compound and mixed overnight. The saturated solution was filtered and quantified against a DMSO stock solution using LC-UV. ^b Permeability assay in MDCK (MDR1) cells. Direction is indicated by A₂B or B₂A. ER denotes efflux ratio. ND denotes not determined. ^c r/d/h denotes rat, dog or human derived plasma protein/microsomes/hepatocytes respectively.

The trifluorobutyl **20** and pyran **23** both exhibited acceptable permeability and microsomal half-lives (**Table 6**). In the case of compound **20**, acceptable hepatocyte half-lives were observed in all species. Unbound protein fractions were good for both compounds and thermodynamic solubility was improved versus the iso-pentyl **14**. As a result, both these compounds were progressed into *in vivo* pharmacokinetic evaluation, this data is shown in **Table 8** *vide infra*. The trifluorobutyl substituted 7-fluorooxindole system **21**

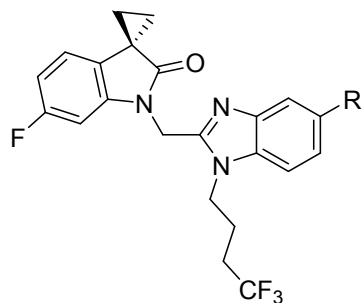
1
2
3 had shown favorable *in vitro* ADME properties and acceptable potency
4
5 (**Table 5**). In this case, low oral bioavailability observed in
6
7 both mouse and rat (12.9% and 14% respectively, **Table 8**). The
8
9 high clearance in mice and rats for **21** was not predicted by the *in*
10
11 *vitro* data. Compound **20** showed lower clearances in mice and dogs
12
13 indicative of an improved metabolic stability in these species.
14
15 High volumes of distribution were observed for both compounds **20**
16
17 and **21**.
18
19
20
21

22 **Aminomethylene substituent modifications**

23
24

25 To complete the investigation into substituent effects in this
26
27 system, a range of modifications were introduced at the 6 position
28
29 of the benzimidazole. Polar, non-polar, basic and acidic groups
30
31 were all investigated at this position (**Table 7**). The potential
32
33 for the interaction of this group in this class of molecule to
34
35 bind to target site acidic amino acid residues has been highlighted
36
37 in earlier publications.²⁸ Our strategy at this stage was to
38
39 investigate alternatives to the aminomethylene, mostly with
40
41 hydrogen bonding potential that could be associated with a
42
43 different pharmacokinetic absorption or stability profile. To
44
45 summarize the output from this program of work, the structure
46
47 activity pattern observed within our system clearly demonstrated
48
49 that basic groups, such as a simple amine or the strongly basic
50
51 amidine functionality, were the most potent (e.g. **25**) and potency
52
53
54
55
56
57
58
59
60

1
2
3 in the fusion assay for these compounds was maintained in the
4 plaque assay. Neutral groups such as amide and methanesulphonyl
5
6 (28 and 30) demonstrated significantly poorer levels of activity
7
8 whilst acidic groups were inactive in this specific scaffold (29).
9
10 In the case of the 6-chlorine substituted analogue 33, reduced
11
12 potency in the plaque assay was compounded by low permeability and
13
14 high clearance in microsomes (table 6). In addition, there was a
15
16 clear trend for simplicity of substituent, with the introduction
17
18 of alkyl groups into the amidine functionality either as a spacer
19
20 group or nitrogen substituent negatively impacting upon activity
21
22 (26 and 27)²⁹. The potency of the amidine containing analogue was
23
24 counteracted by the low absorption characteristics of this
25
26 strongly basic group:³⁰ permeability was low in both directions
27
28 (25: MDCK (MDR1) A₂B:B₂A P_{app} = 0.413:0.876 × 10⁻⁶ cm s⁻¹).
29
30 Subsequently the potential for interaction of such basic
31
32 functionality with a hydrophilic region within the fusion protein
33
34 was supported by the crystal structure obtained for our clinical
35
36 compound (Figure 9).
37
38
39
40
41
42
43
44



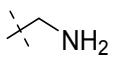
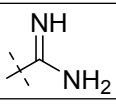
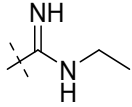
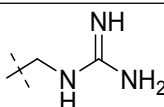
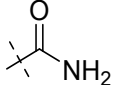
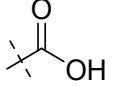
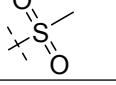
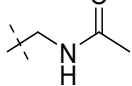
Cmpd	R	RSV Fusion IC ₅₀ (nM)	RSV A2 Plaque EC ₅₀ (nM)	CC ₅₀ (nM)
20		0.9	1.3	5,588 >2000* >4,000**
24	CN	ND	444.2	23,700
25		3	0.5*	>20,000*
26		640.5	453.9	>25,000
27		183.0	21.1*	>20,000*
28		71.0	13.7*	>20,000*
29		>25,000	10,181.3	>25,000
30		1,069.5	3,636.0	>25,000
31		364.5	106.7*	>20,000*
32	H	37.2	17.9	>25000**
33	Cl	6.2	5.4	>25000**

Table 7. Antiviral activity and cell cytotoxicity data for 6-substituted benzimidazoles. The plaque reduction assay (PRA) was performed in Vero cells or Hep2 cells* with the RSV A2 strain. CC₅₀ refers to cell cytotoxicity in HepG2 cells and was assessed by MTT staining. Alternatively, compound cell toxicity was performed in either Hep2 cells* or Vero cells** as described

1
2
3 earlier. IC_{50} , EC_{50} and CC_{50} values are an average of at least 2
4
5 testing occasions.
6
7
8
9

11 **Aza-oxindoles and heterocyclic spiro-oxindole systems**

12
13
14
15 Introduction of nitrogen into the oxindole system had been of
16
17 interest through this optimization period, due to an expectation
18
19 of improved potency associated with the cyclopropyl variant of **7**
20
21 (**Figure 3**) that was identified as a lead compound during the hit
22
23 finding exercise. Synthesis of useful quantities of material to
24
25 allow full profiling of compounds containing this substructure
26
27 proved difficult and these difficulties relegated the priority of
28
29 this work within the optimization program. Two exemplary aza-
30
31 oxindoles (**34** and **35**, **Figure 7**) were prepared which demonstrated
32
33 potency in plaque assays (**34**: $EC_{50} = 2.1$ nM and **35**: $EC_{50} = 4.1$ nM).
34
35 Compound **35** displayed a low intrinsic permeability (MDCK (MDR1)
36
37 $P_{app} A_2B:B_2A = 0.1:0.0 \times 10^{-6}$ $cm s^{-1}$) and high clearance (**Table 6**)
38
39 that translated to low bioavailability in the mouse (18%) with
40
41 high clearance (81 $mL min^{-1} kg^{-1}$, **Table 8**).
42
43
44
45
46
47

48 Our program strategy had from the start utilized the structurally
49
50 novel approach of incorporating a spirocyclic ring system into a
51
52 bicyclic template (**Figure 3**). Although this annotation has focused
53
54 on the spirocyclopropyl output from this exercise, a number of
55
56
57
58
59
60

1
2
3 catch up and overtake the evaluation of RV521. As such the
4
5 compound was held as a short term back up compound in the event of
6
7 issues occurring with RV521. The remainder of the discussion will
8
9 focus on the properties of RV521.
10
11
12
13
14
15

Entry	Species	Dose; iv/po, (mg/kg)	$t_{1/2}$ (po/iv, h)	t_{max} (h) po	C_{max} po (ng/mL)	Cl (iv) (mL/min/kg)	Vd_{ss} (iv) (L/kg)	F (%)
20	Mouse	1/10	4.2/3.1	2.0	224	47.9	17.5	46.4
20	Rat	1/10	1.8/9.9	2.7	74.2	164	22	102
20	Rat	NT/50	ND/5.9	5.3	475	ND	ND	132
20	Dog	0.3/3	12.3/7.4	4.0	82.4	17.8	17.6	44.2
21	Mouse	1/5	2.4 / ND	2.0	110	76	11.3	12.9
21	Rat	1/10	ND / 0.8	2.1	44.3	209	11.0	13.8
22	Mouse	1/10	ND/0.9	0.1	47.8	82.7	3.8	4.4
23	Mouse	1/10	1.7/1.4	1.7	450	58	5.5	39.4
23	Dog	0.3/3	5.2/3.1	0.5	505	19.2	5.0	163
35	Mouse	1/10	ND/1.0	2.0	200	81.1	4.5	18.1

36
37
38
39 **Table 8.** *in vivo* Pharmacokinetic data for leading compounds in
40 multiple species. ND indicates not determined; NT indicates not
41 tested. The compound was dosed as a suspension of the amorphous
42 solid at the doses indicated *iv* and *po*.
43
44
45
46
47
48
49

50
51 RV521 showed a moderate to long intravenous half-life (4.2 h in
52 mice, 1.8 h in rats and 12.3 h in dogs) with variable clearance in
53
54
55
56
57
58
59
60

1
2
3 these species, approximately 53% to 61% of hepatic blood flow in
4 mice and dogs and in contrast, approximately 200% of hepatic blood
5 flow in rats. The compound had a large volume of distribution in
6 all the species tested, suggestive of extensive tissue
7 distribution. Subsequently, the relevance of this property of
8 RV521, and other molecules in this series, was reinforced by repeat
9 oral dosing studies in rats that showed a high lung to plasma ratio
10 for RV521 (see supplementary information). Lung and plasma samples
11 were taken on day seven (4 hr and 24 hr timepoints) of a repeat
12 dosing study, QD at 43.5mg/kg. Analysis of these samples showed
13 a 100-fold and 500-fold lung to plasma ratio. RV521 was present in
14 the lung at a concentration of 11.8 mg/g at this dose at the 24-
15 hour timepoint on day 7.

16
17 Oral exposure was demonstrated in rats at doses of 10 and 50 mg/kg
18 with bioavailability at 102% and 132%, respectively: the apparent
19 availability >100% most likely due to dose-dependent non-linear
20 kinetics. Plasma concentrations in rats declined with a half-life
21 of 3.1 hours and the compound was absorbed relatively slowly with
22 a t_{\max} of 5.3 hours. When dogs were dosed at 3 mg/kg, the
23 bioavailability was shown to be 44.2%, with an oral $t_{1/2}$ of 12.3
24 hours and the compound was absorbed relatively slowly with a t_{\max}
25 of 4 hours. An evaluation of metabolism in primary hepatocytes
26 suggested that hepatic metabolism was a major pathway of
27 elimination across all these species.

1
2
3 The activity of RV521 in RSV plaque assay was evaluated against a
4 panel of laboratory strains and low passage clinical isolates of
5 RSV A and B strains. RV521 showed potent activity, with an average
6 IC_{50} of 1.4 nM for RSV A (n=20) and 1.0 nM for RSV B (n=16) (see
7 supplementary information for strains tested against and IC_{50} s).

8
9
10
11
12
13
14
15 The inhibition of RSV by RV521 was further investigated in an *in*
16 *vitro* primary human airway epithelial cell (HAE) infectivity
17 model.²⁵ The use of HAE cells provided a closer clinical context
18 for RSV evaluation than that possible by standard plaque assay
19 formats in continuous cell lines. Further, the use of trans-well
20 plate inserts in this system allows for apical infection of the
21 system with virus whilst allowing dosing the compound
22 basolaterally, a system reflective of systemic exposure (**Figure**
23 **8**). Differentiated HAE cell cultures mimic certain aspects of
24 infection pathology and unlike rodent models which are only semi-
25 permissive to infection, retain replicative capacity. This model
26 has been used previously in the testing of RSV N protein
27 inhibitors.³³ Recently the differential activities of RSV
28 inhibitors in the human airway epithelium model has been
29 reported.³⁴

30
31
32
33
34
35
36
37
38
39
40
41
42
43
44
45
46
47
48
49
50
51
52
53
54
55
56
57
58
59
60

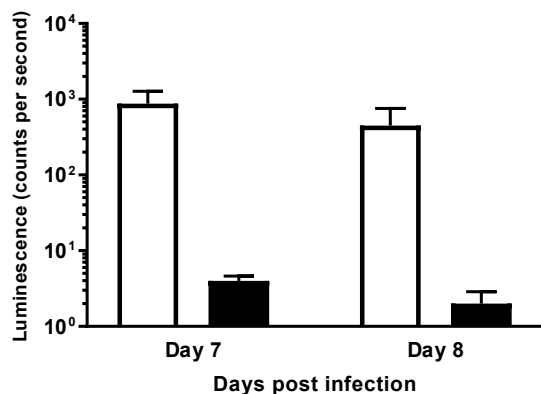


Figure 8a. RV521 inhibition of RSV infection of HAE cells. Treatment of HAE cells with 10 nM RV521 2 h prior to infection (shaded bars) with recombinant luciferase-expressing RSV reduced the titre (as measured by luminescence) at 7 and 8 days post infection versus untreated controls (white bars). Data are presented as mean \pm SD (n=3).

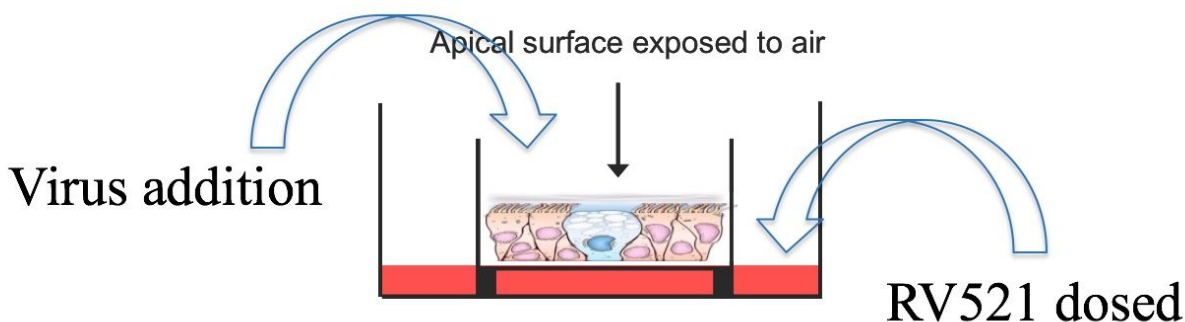


Figure 8b. Representation of the insert cell system that allows viral infection to and sampling of the apical surface of the epithelial layer and compound administration (blue arrows) to the basolateral surface of the cells via the cell nutrient (salmon).

1
2
3 Treatment of HAE cells with 10 nM of RV521 resulted in a
4
5 significant reduction in RSV shed from the apical surface compared
6
7 to untreated controls. As shown in **Figure 8**, 2.30 log₁₀ and 2.35
8
9 log₁₀ reductions in RSV titre compared with untreated controls were
10
11 observed on day 7 and day 8 post infection, respectively.
12
13
14
15
16
17
18
19
20
21
22
23
24
25
26
27
28
29
30
31
32
33
34
35
36
37
38
39
40
41
42
43
44
45
46
47
48
49
50
51
52
53
54
55
56
57
58
59
60

Histological analysis of the control and compound treated HAE cell cultures, at 8 days post infection, revealed that control and compound treated cells retained tight junctions, suggestive of a healthy epithelial cell layer and RV521 treatment did not elicit any apparent change in cell morphology or viability.

In order to characterize the mode of action of RV521 and to identify the viral determinants conferring reduced susceptibility to RV521, we performed an *in vitro* resistance selection study.

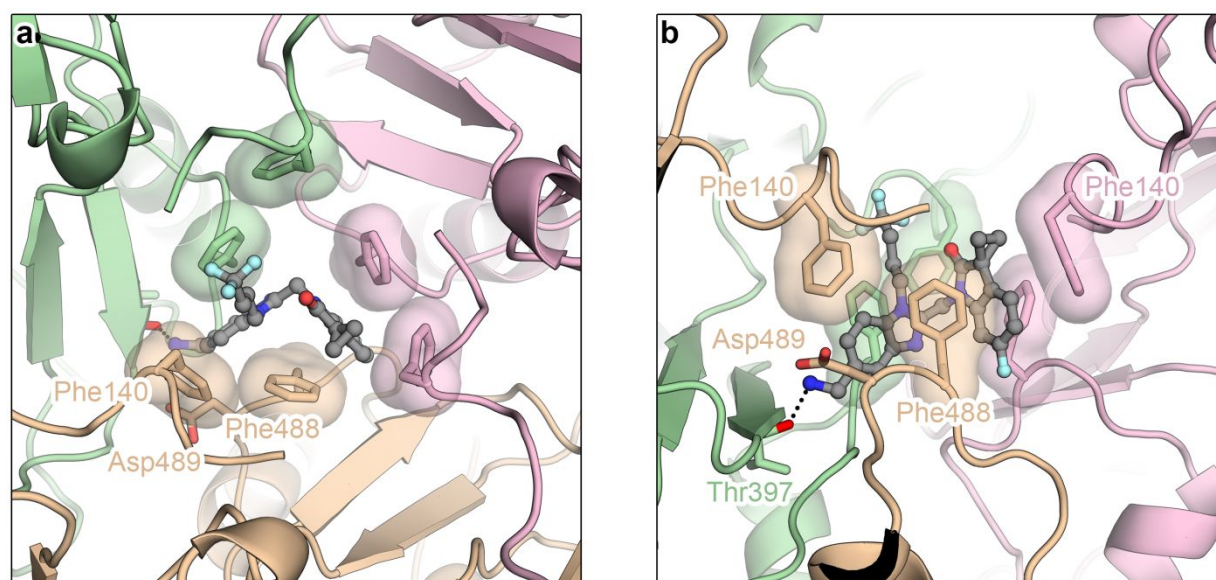
An RSV stock resistant to RV521 was generated by serial passage of RSV in increasing concentrations of RV521. We utilized Hep-2 cell cultures inoculated with RSV strain Memphis 37b in the presence of RV521 (at IC₅₀ concentration) or no inhibitor (control). Once an 80-90% cytopathic effect was observed, or after a maximum of 7 days, RSV was passaged into fresh HEp2 cells and the concentration of RV521 increased 2-fold. Serial passaging in the presence of increasing concentrations of RV521 was continued for ten passages. The resistant RSV stocks were used for EC₅₀ determinations by plaque assay, and RNA was extracted for RSV F gene sequencing. This

1
2
3 identified an amino acid substitution at position 489 in the RSV
4 F protein, aspartic acid (D) to tyrosine (Y) (D489Y) with
5 resistance to RV521. EC₅₀ values for RV521 against the RV521
6 resistant virus and passage control virus were 88.98 nM and 1.18
7 nM, respectively, representing a 76-fold shift in IC₅₀ in response
8 to the acquisition of viral resistance to RV521.
9

10
11
12 D489Y is a mutation in the RSV F protein observed in *in vitro*
13 resistance studies with other RSV fusion inhibitors^{35 - 37} and cross
14 resistance with these inhibitors of RSV fusion was observed (see
15 supplementary information). The resistant virus remained sensitive
16 to treatment with known RSV replication inhibitors, the N-protein
17 inhibitor RSV604 and the nucleoside pro-drug ALS-8112. However,
18 most importantly, RSV containing D489Y has shown to have reduced
19 fitness, with the virus exhibiting poor growth characteristics, in
20 culture.^{37, 38}
21
22
23
24
25
26
27
28
29
30
31
32
33
34
35
36
37

38 We were able to obtain a crystal structure of RV521 bound to the
39 pre-fusion conformation of the F protein (**Figure 9**). This
40 structure placed the compound into the central binding region
41 defined by subunits of the trimeric protein as described for other
42 fusion inhibitors, notably that described for JNJ-53718678.³⁷ Key
43 interactions observed are π interactions with the three key
44 phenylalanine residues in this trimer defined pocket. Phe140 and
45 Phe488 from one monomer shown in gold in Figure 9a and Phe140 from
46
47
48
49
50
51
52
53
54
55
56
57
58
59
60

1
2
3 a second monomer define these interactions. The aminomethylene
4 functionality was observed to form a potential H bond with Thr397
5 from the third monomer (**Figure 9b**). The mutable aspartic acid
6 D489 was observed as a close neighbor of the amino group of RV521
7 from the third monomer (**Figure 9b**). The mutable aspartic acid
8 D489 was observed as a close neighbor of the amino group of RV521
9 with an N-H to C=O distance of around 2.6Å. This observation was
10 strongly supportive of the requirement for basic group in the
11 inhibitor.
12
13
14
15
16
17
18
19

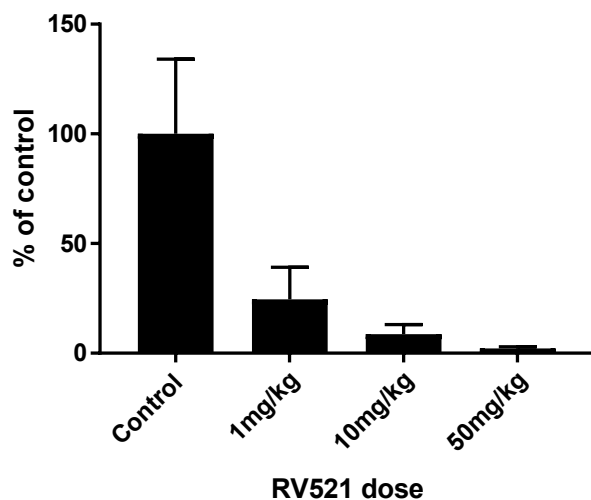


38 **Figure 9.** Crystal structure of RV521 bound to the F-protein (PDB
39 code 7KQD) in its trimeric pre-fusion conformation. Views are
40 shown of the binding site created by the trimer. Amino acid
41 residues are shown as gold, pink or green filled sticks with the
42 backbone shown as a ribbon in the corresponding color. Each
43 colored region corresponds to each individual monomer. **a)** Binding
44 mode in a top-down view of RV521 depicting π bonding interactions
45 with phenylalanine 488 and 140 of the gold monomer. **b)** Binding
46
47
48
49
50
51
52
53
54
55
56
57
58
59
60

1
2
3 mode showing the orientation of the aminomethylene into a
4 hydrophilic region created by Asp489 and Thr397 with the H bonding
5 interaction with Threonine 397 backbone carbonyl indicated by the
6 dotted line. The proximity of the mutable Asp489 is depicted most
7 clearly in panel b. Amino acid residue labels are shown in the
8 colour of the monomer.
9

10
11
12 Final support for the progression of the compound to the clinic
13 was provided by an *in vivo* efficacy evaluation of RV521 in Balb/C
14 mice inoculated with RSV A2 (**Figure 10**). A number of animal models
15 exist for this evaluation of compounds *in vivo* however they are of
16 varying utility, most notably in terms of compound requirement.²⁶
17
18 In our case, mice received two oral doses of RV521 (0, 1, 10 or 50
19 mg/kg) 2 hours pre- and 24 hours post intranasal inoculation with
20 RSV strain A2. Animals were euthanized 5 days post RSV inoculation
21 and lung homogenates prepared. Viral titres in lung homogenates
22 were evaluated by plaque assay on Vero cells. Virus titres in the
23 lungs of mice treated with 50, 10 and 1 mg/mL RV521, compared to
24 the control group, were reduced by 1.6 log₁₀ (98% reduction), 1.09
25 log₁₀ (92% reduction) and 0.67 log₁₀ (79% reduction), respectively.
26
27 Concentrations of RV521 were measured in plasma samples taken 5
28 hours after the first dose and immediately prior to the second
29 dose of the compound. Concentrations of RV521 measured in the
30 plasma were vastly in excess of EC₅₀ figures (see supplementary
31
32
33
34
35
36
37
38
39
40
41
42
43
44
45
46
47
48
49
50
51
52
53
54
55
56
57
58
59
60

1
2
3 information) except at the lowest dose. The activity of the
4
5 compound observed in this model at the 1mg/kg dose has to be taken
6
7 in the context of the distributive properties of the compound *vide*
8
9 *infra*.

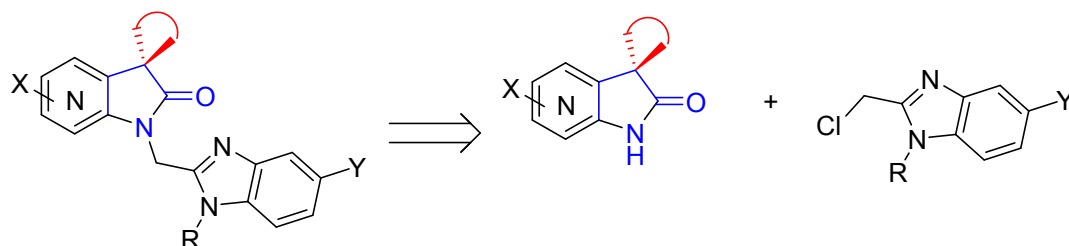


10
11
12
13
14
15
16
17
18
19
20
21
22
23
24
25
26
27
28
29
30
31
32 **Figure 10.** RV521 reduced lung virus titres in a Balb/C mouse
33 model of RSV infection. Balb/C mice were treated with RV521 (1, 10
34 or 50 mg/kg) 2 hours pre- and 24 hours post intranasal inoculation
35 with RSV strain A2. RSV viral titres in lung homogenates were
36 measured 5 days post infection. Data are expressed as a percentage
37 of control group and shown as mean \pm sd (n=6 animals per group).
38
39
40
41
42
43
44
45
46
47
48

49 **Synthesis Overview**

50
51
52 In general, compounds prepared within this program utilized the
53 same convergent synthetic strategy with benzimidazole and
54
55
56
57
58
59
60

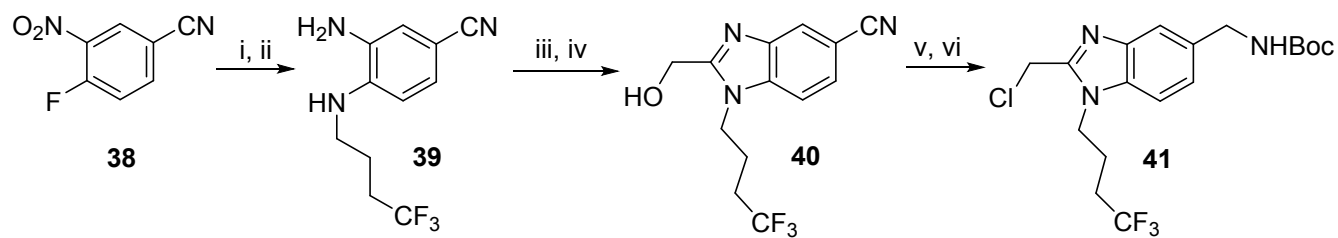
1
2
3 spirocyclic oxindole fragments prepared as key intermediates
4
5 (**Scheme 1**). These two fragments were then linked via alkylation
6
7 of the spirocyclic lactam.
8
9



19 **Scheme 1.** Disconnection of generalized target compound structure
20
21 into chlorobenzimidazole and spirocyclic intermediates. Blue and
22
23 red rings indicate variable sized spirocyclic ring systems. X =
24
25 F, Cl, H. Y = H, CH₂NHBoc, Cl, CN. R is a variable alkyl chain.
26
27
28

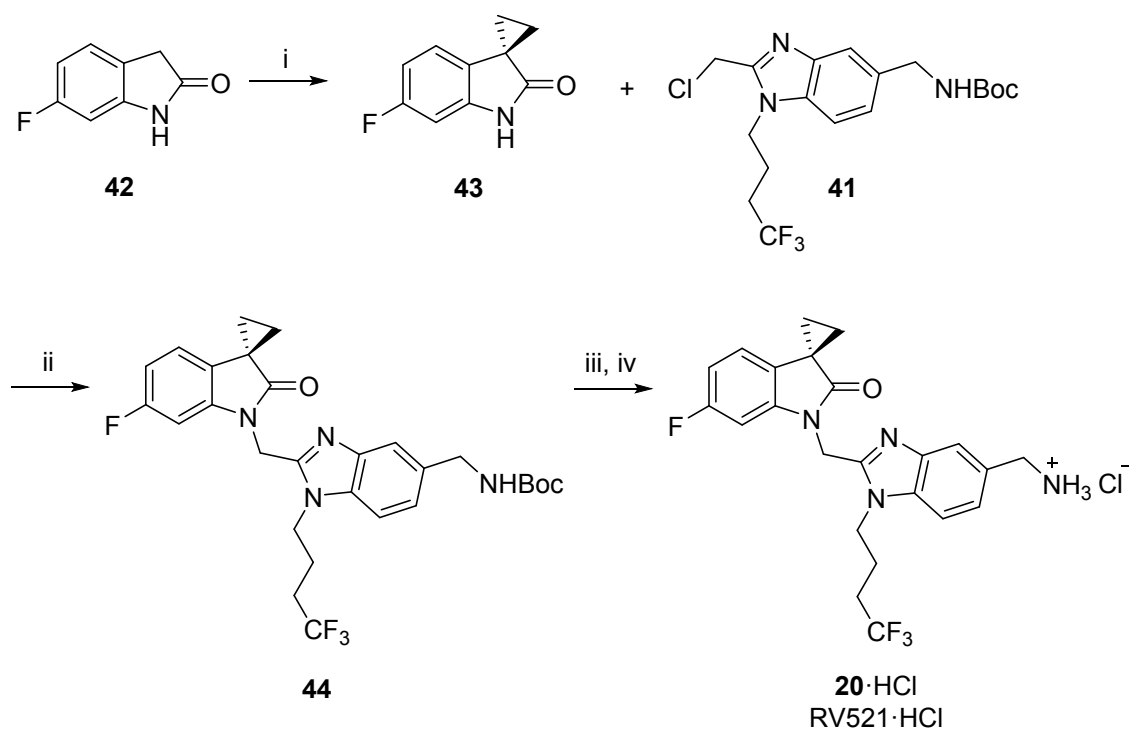
29 The discovery phase synthesis of RV521 is representative of the
30
31 route employed for the preparation of the benzimidazole
32
33 intermediates (**Scheme 2** and **Scheme 3**). This proceeded via an
34
35 established sequence which started with an S_NAr displacement of
36
37 the chlorine of 4-chloronitrobenzotrile **38** by
38
39 trifluorobutylamine. Nitro reduction, benzimidazole formation
40
41 with the chloroacetyl chloride and acetate hydrolysis provided
42
43 nitrile **40**. Nitrile reduction and subsequent chlorination
44
45 provided the key chloromethyl intermediate **41** (**Scheme 2**).¹⁸
46
47
48
49 Cyclopropanation of 6-fluorooxindole **42** was performed utilizing
50
51 lithium diisopropylamide as base in an alkylation methodology with
52
53 1,2-dibromoethane to provide the spirocyclopropyl oxindole **43**.
54
55
56
57
58
59
60

Both halves of the molecule (**41** and **43**) were then linked via a simple displacement reaction (**Scheme 3**). Removal of the BOC protecting group and hydrochloride salt formation afforded a clean preparation of the HCl salt of RV521.³⁹



Scheme 2. Synthesis of benzimidazole intermediate for RV521.

Reagents and conditions: i) 4,4,4-trifluorobutan-1-amine, NEt_3 , MeCN, rt, 16 h, 92%. ii) Pd/C, H_2 , rt, 16 h, 88%. iii) acetoxyacetyl chloride, NEt_3 , CH_2Cl_2 , rt, 2 h, then AcOH, 80 °C, 16 h, 69%. iv) K_2CO_3 , MeOH, rt, 1 h, 91%. v) $\text{Pd}(\text{OH})_2/\text{C}$, HCl, H_2 , MeOH/THF, rt, 16 h, then BOC anhydride, DIPEA, CH_2Cl_2 , rt, 3 h, 83%. vi) MsCl, DIPEA, THF, rt, 16 h, 96%.

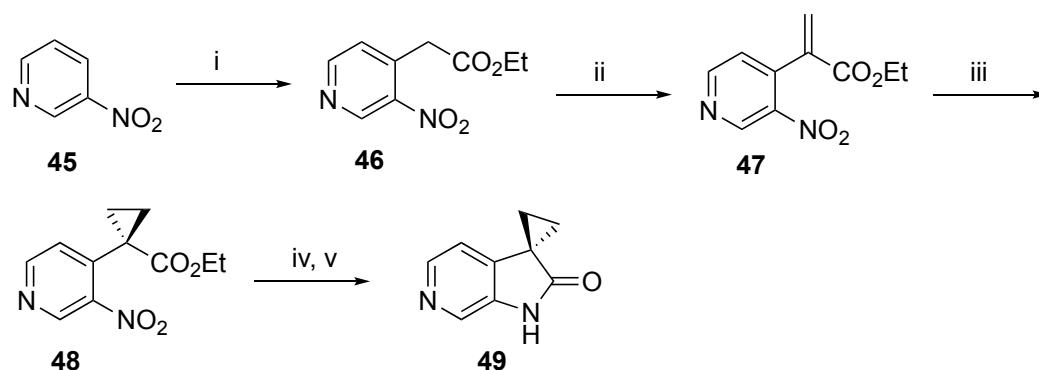


Scheme 3. Synthetic sequence used in the preparation of RV521.

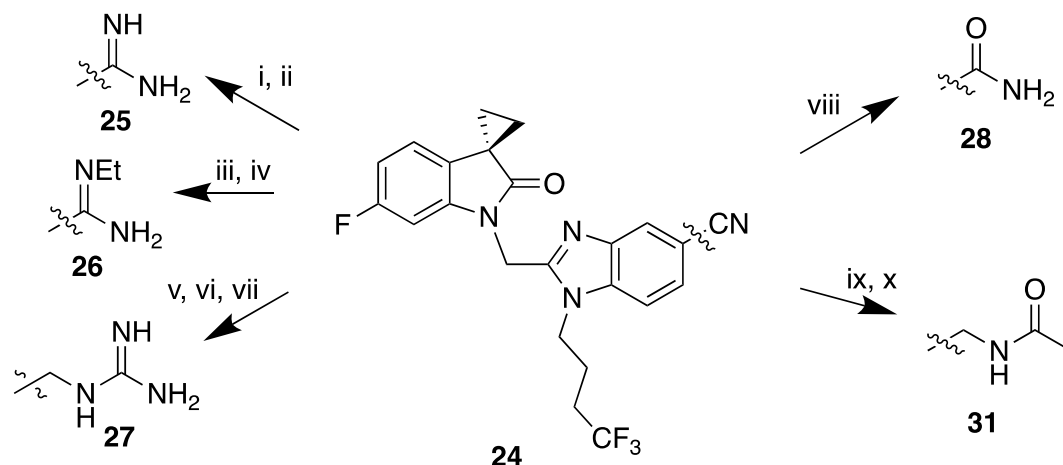
Reagents and conditions: i) *n*-BuLi, diisopropylamine, 1,2-dibromoethane, -40 to 18 °C, 47%. ii) NaH, DMF, rt, 16 h, 75%. iii) HCl (2 M in Et₂O), CH₂Cl₂, rt, 6 h, then aq. NaHCO₃ workup, 63%. iv) HCl (2 M in Et₂O), CH₂Cl₂, 30 min, 81%.

Other benzimidazole precursors were prepared via an analogous sequence to that shown for the synthesis of **20** (and are detailed in the supporting information), while the spirocyclic lactams employed in the hit finding exercise could be prepared via an alkylation methodology to construct the exocyclic ring last, with a complementary approach enabling preparation of a spirocyclic 6,6-system (details in supporting information).⁴⁰ Recently

developed cyclopropanation methodologies have been reported that enable facile one-pot access to the spirocyclopropyl oxindoles of compounds **11-17** and **35** without N-protection.^{41, 42} Of particular note, the nucleophilic alkylation methodology of Andreasson *et al.* was exploited to enable construction of the spirocyclopropyl azaoxindole **49** (Scheme 4).⁴³ Addition of a methylene to the pyridyl acetoacetate **46** afforded **47**. Subsequent cyclopropanation to **48** was followed by nitro reduction and ring closure to give the target oxindole **49**. 6-Substituted benzimidazole target compounds were assembled either directly from **20** or via manipulation of the 6-cyano analogue **24** (Scheme 5).



Scheme 4. Synthesis of spirocyclic azaoxindole **49**. Reagents and conditions: i) Ethylchloroacetate, KO^tBu, 0 °C to rt, 2.5 h, 80%. ii) K₂CO₃, benzyltriethylammonium chloride, paraformaldehyde, toluene, 90 °C, 1.25 h, 77%. iii) DBU, trimethylsulfoxonium chloride, CH₃CN, 60 °C, 45 min, 59%. iv) Pd/C, EtOH, H₂, 16 h. v) 1,5,7-triazabicyclo[4.4.0]dec-5-ene, 80 °C, 1 h, 90%.



Scheme 5. Synthesis of 6-aminomethylene derivatives from 6-cyanobenzimidazole **24** (Synthesis described in supplementary information). *Reagents and conditions:* **25:** i) acetyl chloride, EtOH, rt, 16 h. ii) NH₃, methanol, rt, 48 h, 21%. **26:** iii) acetyl chloride, EtOH, rt, 16 h. iv) EtNH₂, methanol, rt, 16 h, 57%. **27:** v) 5% Pd/C, H₂, HCl/MeOH, 77%. vi) (BocN)₂C=N(SO₂CF₃), Et₃N, CH₂Cl₂, rt, 23 h. vii) TFA, CH₂Cl₂, rt, 19 h. 78%. **28:** viii) NaOH, dioxane, reflux, 36%. **31:** ix) 5% Pd/C, H₂, HCl/MeOH, 77%. x) acetyl chloride, NEt₃, CH₂Cl₂, rt, 16 h, 71%.

RSV521 Progression into Clinical Trials

RV521 progressed into the pre-clinical evaluation phase utilizing a virtual development model employing external contract synthesis, pharmacology and toxicology. In summary, *in vitro* broad receptor

1
2
3 pharmacology was acceptable and the cardio toxicology profile
4 exhibited no QT effects in an anaesthetised guinea pig model or
5 subsequently in any *in vivo* (dog telemetry) studies. Ames and rat
6 micronucleus tests were negative. Single dose safety pharmacology
7 showed no evidence of any toxicology and repeat dose studies in
8 rats and dogs determined a NOAEL of 45 mg/kg/day with all events
9 observed at higher doses found to be reversible. Rats were dosed
10 up to 240mg/kg and dogs to 120mg/kg in single dose studies. Repeat
11 dose studies were for 28 days, dosing once daily at 120mg/kg/day
12 in rats and 45mg/kg/day in dogs. The dose predictions for the
13 first study in man were based on *in vitro* clearance values in rat.
14 On this basis, and assuming a one-compartment first-order
15 absorption model, daily oral doses of 50 mg were predicted to
16 achieve steady state trough concentrations equivalent to a 3-fold
17 margin above the *in vitro* EC₉₀ value for total (free and bound)
18 plasma concentration of RV521.
19
20
21
22
23
24
25
26
27
28
29
30
31
32
33
34
35
36
37
38
39

40 Subsequent evaluation of PK from the initial Phase 1 study in
41 healthy volunteers indicated that the predictions based on rat
42 clearance overestimated RV521 plasma exposure and doses of 200mg
43 and 350mg bid were required to meet or exceed the target of a 3-
44 fold margin above the *in vitro* EC₉₀ value.
45
46
47
48
49
50

51 The path through the initial stages of clinical development has
52 become established for inhibitors of RSV primarily because of the
53
54
55
56
57
58
59
60

1
2
3 availability of an RSV challenge virus. In general, small-molecule
4 inhibitors of RSV have progressed through the clinic according to
5 draft EMEA guidelines.^{44, 45} In general, after Phase 1 single and
6 multiple ascending dose studies in healthy volunteers to
7 demonstrate safety, tolerability, and indicate pharmacokinetics,
8 clinical compounds have entered a Phase 2a proof of concept study
9 in the human challenge model. This is a trial whereby cohorts of
10 healthy volunteers are quarantined in a specialist unit and
11 intranasally infected with RSV strain Memphis 37b, the only GMP
12 quality RSV virus currently available for human challenge. Viral
13 load, as assessed by assay of nasal washes, has been shown to
14 correlate with disease severity in the challenge model⁴⁶ and
15 treatment is delayed until volunteers are shedding virus, this
16 model therefore formed a basis whereby the effect of antiviral
17 agents can be studied in a well-controlled patient group.
18
19
20
21
22
23
24
25
26
27
28
29
30
31
32
33
34
35
36
37
38

39 Data from RSV fusion inhibitors studied in this clinical model has
40 been published. Presatovir and JNJ-53718678 (**1** and **2**, **Figure 1**)
41 were shown to effectively reduce viral load and reduce symptom
42 scores.^{11, 47} Subsequently with this proof of concept in hand,
43 inhibitors have moved into patient population studies. The initial
44 patient studies being in pediatric populations, targeting infants
45 up to the age of 24 months. In cases where toxicology of a compound
46 has not supported progression in infants,⁴⁸ the next stage of
47
48
49
50
51
52
53
54
55
56
57
58
59
60

1
2
3 evaluation has been in vulnerable adult populations such as
4
5 hematopoietic cell transplant (HCT) recipients with RSV infections
6
7 of the upper or lower respiratory tract (URTI or LRTI), lung
8
9 transplant patients with RSV infection and adults hospitalized
10
11 with RSV infections.⁴⁹⁻⁵¹
12
13

14 Significant challenges are associated with both of these clinical
15
16 evaluation routes. Aside from recruitment issues, adult
17
18 populations can be highly variable due to multiple clinical sites
19
20 being required to ensure patient numbers. Pediatric clinical
21
22 studies require a revisiting of ascending dose studies prior to
23
24 any patient study and the disease course in pediatric patients is
25
26 quite different to that in adults. Essentially infants struggle to
27
28 control primary RSV infections and lower age trends toward slower
29
30 viral clearance and a greater viral load, as measured by viral
31
32 AUC.⁵²
33
34
35

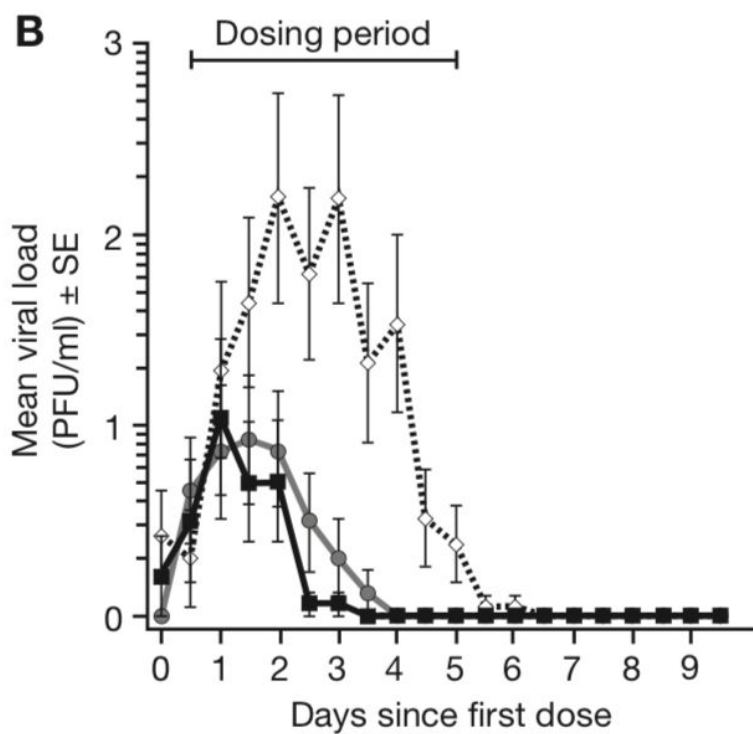
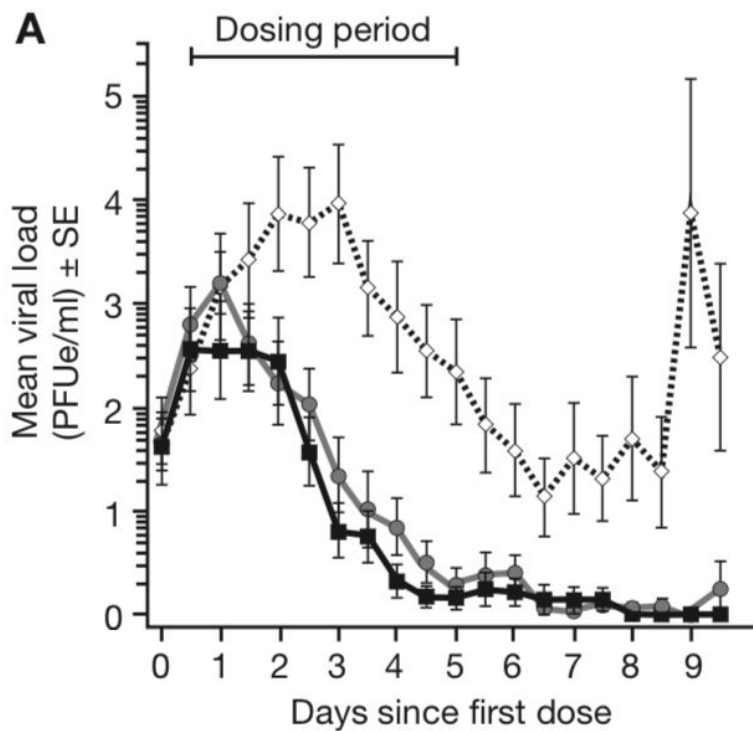
36
37 RV521 progressed through phase 1 single ascending and multiple
38
39 ascending dose studies in a total of 76 healthy volunteers. At
40
41 doses between 175 mg and 350 mg, exposures could be achieved that
42
43 provided trough levels greater than a multiple of three times the
44
45 plasma protein adjusted EC_{90} . (this was the median EC_{90} from
46
47 multiple (n=16) RSV plaque assays with RSV strain A2). No serious
48
49 adverse events were reported at the doses investigated and this
50
51 allowed the dosing regimen to be formulated for the progression of
52
53 the compound into the human challenge model.
54
55
56
57
58
59
60

1
2
3 The Phase 2a clinical study⁵³ was performed to establish proof-of-
4 concept for the antiviral activity of RV521 in the treatment of
5 RSV, using a virus challenge model per regulatory guidance.
6
7 Additional aims for this study were to determine the safety,
8 tolerability, and pharmacokinetic profile of RV521 and to perform
9 mutation detection analyses to test for potential development of
10 RSV resistance to RV521.⁴⁵

11
12 The study was conducted in healthy male or female adult volunteers
13 (aged between 18 and 45 years), with low serum levels of pre-
14 existing specific antibodies to RSV, which indicated that the
15 subject would be sensitive to RSV infection and would likely become
16 infected following inoculation with the challenge virus. This
17 challenge virus was the RSV-A Memphis 37b strain and approximately
18 4 log₁₀ plaque forming units (PFU) were administered on day zero.
19 Subjects were then randomly assigned to three equivalently sized
20 groups and dosed with 200 mg, or 350 mg of RV521, or placebo twice
21 daily for 5 days following confirmation of infection.

22
23 Nasal wash samples were taken twice daily from day 2 through to
24 discharge (day 12), to allow measurement of viral load via reverse
25 transcriptase quantitative RT-qPCR and a cell-based infectivity
26 assay.⁵³ The occurrence and severity of symptoms were reported, and
27 nasal mucus weighed. Pharmacokinetic assessments were based on
28 venous blood samples, taken from day zero through to discharge.
29 Safety assessments including electrocardiogram recordings,
30
31
32
33
34
35
36
37
38
39
40
41
42
43
44
45
46
47
48
49
50
51
52
53
54
55
56
57
58
59
60

1
2
3 physical examination and urinalysis were taken at prespecified
4
5 timepoints throughout the study. Adverse events were monitored
6
7
8 daily.
9
10
11
12
13
14
15
16
17
18
19
20
21
22
23
24
25
26
27
28
29
30
31
32
33
34
35
36
37
38
39
40
41
42
43
44
45
46
47
48
49
50
51
52
53
54
55
56
57
58
59
60



■ RV521 350 mg (N = 16)
● RV521 200 mg (N = 18)
◇ Placebo (N = 19)

1
2
3 **Figure 21.** Mean viral load by nasal wash RT-qPCR (A) and by nasal
4 wash cell-based infectivity assay (B) by day relative to dosing.
5
6
7 Once RSV infection was confirmed treatment was initiated at 200 mg
8 or 350 mg b.i.d. Viral load (RT-qPCR) appeared to rebound after
9
10 day 8.5 in the placebo arm. However, this apparent increase
11
12 resulted from the staggered randomization of subjects (the mean
13
14 viral load at day 9 was calculated from just four subjects, three
15
16 of whom had consistently high viral loads throughout the study).
17
18
19 Figure reprinted under a Creative Commons Attribution 4.0
20
21 International Licence (CC BY 4.0).⁵³
22
23
24
25

26
27 Reprinted from DeVincenzo, J.; Tait, D.; Efthimiou, J.; Mori, J.; Kim, Y.-I.; Thomas, E.; Wilson,
28
29 L.; Harland, R.; Mathews, N.; Cockerill, S.; Powell, K.; Littler, E. A Randomized, Placebo-
30
31 Controlled, Respiratory Syncytial Virus Human Challenge Study of the Antiviral Efficacy, Safety,
32
33 and Pharmacokinetics of RV521, an Inhibitor of the RSV-F Protein. *Antimicrob. Agents*
34
35 *Chemother.* 2020, 64, e01884-19. Copyright 2020 American Society of Microbiology.
36
37
38
39

40
41 Efficacy data for mean viral loads versus time are shown in **Figure**
42
43 **11a** and **Figure 11b**. There was a significant reduction in the mean
44
45 AUC of viral load as assessed by RT-qPCR and cell-based infectivity
46
47 assay with RV521 versus placebo for both doses of RV521. The
48
49 percentage reduction highlighted the scale of this effect with the
50
51 mean reductions in RT-qPCR AUC for RV521 at 200 mg and 350 mg
52
53 relative to placebo calculated at 55.25% and 63.05%, respectively,
54
55
56
57
58
59
60

1
2
3 and 76.42% and 68.60% reduction by cell-based infectivity assay.
4
5 RV521 at these doses significantly reduced the AUC of total symptom
6
7 score compared with placebo and a post-hoc analysis of nasal mucus
8
9 weight data showed that the mean daily nasal mucus weight was
10
11 significantly lower in the RV521 treatment groups relative to
12
13 placebo group. Target group mean trough levels ($3 \times$ plasma protein
14
15 adjusted *in vitro* EC₉₀) were achieved and were maintained at a
16
17 level equivalent or greater than this for the duration of the
18
19 study. The target exposure level was achieved in both dose groups
20
21 with no significant differences in efficacy observed between the 200 mg and 350 mg dose groups,
22
23 although it should be noted that the study was not designed to assess differences in treatment effect
24
25 between the two doses. The most common treatment-emergent adverse events (nausea and
26
27 diarrhea) were mild, transient and resolved. No treatment-related serious adverse events were
28
29 observed. In summary, this clinical human challenge study demonstrated proof of concept for
30
31 clinical efficacy of RV521.
32
33
34
35
36
37
38

39 CONCLUSION

40
41
42 Herein we have described the properties of and process behind the
43
44 identification of **20**, known as RV521 and subsequently named
45
46 sisunatovir, as a potent and clinically efficacious inhibitor of
47
48 RSV fusion in the human challenge model of RSV infection.
49
50
51

52
53 RSV521 was shown to be potent against a panel of RSV A and B
54
55 clinical isolates. Resistance studies confirmed the mode of action
56
57
58
59
60

1
2
3 with key mutations identified and *in vivo* antiviral efficacy was
4 demonstrated in the Balb/C mouse model of RSV infection at levels
5 comparable with those seen for other inhibitors⁵³. Additionally,
6 an effective demonstration of activity was seen in human airway
7 epithelial cells. Oral bioavailability in preclinical species
8 ranged from 42% to >100%, with evidence of efficient penetration
9 into lung tissue. Following a successful pre-clinical phase, the
10 compound progressed through phase one healthy volunteer single and
11 multiple dose studies. In healthy human volunteers experimentally
12 infected with RSV, a potent antiviral effect was observed with a
13 significant reduction in viral load and reduction in symptoms
14 compared to placebo. In conclusion, a potent, oral RSV fusion
15 inhibitor with the potential to treat RSV infection in infants and
16 adults is reported.
17
18
19
20
21
22
23
24
25
26
27
28
29
30
31
32
33
34
35

36 This program to identify RV521 has been core to the progress of
37 the ReViral Ltd. and was supported by a number of funding
38 initiatives. A discussion of the background to the process is of
39 some worth at this stage in the article. The plans for the
40 project were laid by the founding team of ReViral and this led to
41 the initial lead compound **6**. The properties of this compound were
42 sufficient, in terms of absorption and distribution particularly,
43 to allow progression into the lead optimization phase.
44 Identification of RV521 was supported by Reviral and allowed the
45
46
47
48
49
50
51
52
53
54
55
56
57
58
59
60

1
2
3 elevation of the compound into full clinical evaluation. As the
4
5 compound continues to move through clinical evaluation, the
6
7 company has continued to grow, building a pipeline of projects in
8
9 addition to this initial flagship project.
10
11
12

13 EXPERIMENTAL

14
15
16 **General Synthetic Protocols.** All reagents were purchased from
17
18 commercial suppliers and were of the highest available purity.
19
20 Unless otherwise stated, chemicals were used as supplied without
21
22 further purification. Anhydrous solvents were purchased from Acros
23
24 (AcroSeal™) or Sigma-Aldrich (SureSeal™) and were stored under
25
26 nitrogen. Petroleum ether refers to the fraction with a boiling
27
28 point between 40 °C and 60 °C. All reactions were carried out under
29
30 a nitrogen atmosphere, unless otherwise specified. Flash column
31
32 chromatography was performed using an automated chromatography
33
34 system on silica gel. ¹H NMR and ¹³C NMR spectra were typically
35
36 recorded on a Varian VNMRs 500 MHz spectrometer at 30 °C, using
37
38 residual isotopic solvent as an internal reference. The chemical
39
40 shift data for each signal are given as δ in units of parts per
41
42 million (ppm). LC-MS data was recorded on a Shimadzu Prominence
43
44 Series coupled to a LCMS-2020 ESI mass spectrometer. Samples were
45
46 eluted through a Phenomenex Gemini C18 (pore size: 110 Å; particle
47
48 size: 5 μm; dimensions: 250 mm × 4.6 mm column), using water and
49
50 acetonitrile acidified by 0.1% formic acid at 1 mL/min, a run time
51
52
53
54
55
56
57
58
59
60

1
2
3 of 7 min unless otherwise noted and detection at 254 nm. HRMS (ESI)
4
5 was recorded on either a Bruker Daltonics, Apex III, ESI source:
6
7 Apollo ESI, with methanol as spray solvent or a QToF Premier,
8
9 Waters machine (diode array detection: 210-500 nm, oven
10
11 temperature: 40 °C, MassLynx v4.1 data handling) equipped with a
12
13 Waters BEH C18 column (particle size: 1.7 µm; 2.1 × 100 mm) eluting
14
15 with 0.1% formic acid in water and methanol gradient. Only
16
17 molecular ions, fractions from molecular ions and other major peaks
18
19 are reported as *m/z* ratios. The purity of final compounds was
20
21 determined to be >95%, using UHPLC analyses performed on a Waters
22
23 Acquity UPLC system with a Kinetex C18 column (pore size: 100 Å;
24
25 particle size: 1.7 µm; dimensions: 2.1 × 50 mm).

31 **3-Amino-4-(4,4,4-trifluorobutylamino)benzotrile (39)**

32
33 A solution of 4-chloro-3-nitro-benzotrile (10 g, 54.78 mmol),
34
35 4,4,4-trifluorobutan-1-amine (6.91 mL, 60.25 mmol) and NEt₃ (9.16
36
37 mL, 65.73 mmol) in MeCN (130 mL) was stirred at rt for 16 h.
38
39 Further 4,4,4-trifluorobutan-1-amine (0.6 mL, 5.23 mmol) and NEt₃
40
41 (0.9 mL, 6.46 mmol) were added, and the reaction was stirred at rt
42
43 for 5 h. The volatiles were removed *in vacuo*, the residue was taken
44
45 up in water, and the resultant precipitate filtered, washed with
46
47 water, and dried. Trituration with petroleum ether afforded 3-
48
49 nitro-4-(4,4,4-trifluorobutylamino)benzotrile as a bright
50
51 yellow solid (13.71 g, 92%), which was used without further
52
53 purification. ¹H NMR (500 MHz, CDCl₃) δ 8.54 (d, *J* = 2.1 Hz, 1H),
54
55
56
57
58
59
60

1
2
3 8.41 (s, 1H), 7.65 (dd, $J = 9.0, 2.1$ Hz, 1H), 6.92 (d, $J = 8.9$ Hz,
4 1H), 3.49 (q, $J = 6.7$ Hz, 2H), 2.28 (ddt, $J = 15.3, 10.6, 5.5$ Hz,
5 2H), 2.05 (p, $J = 7.5$ Hz, 2H).
6
7
8
9

10 A solution of 3-nitro-4-(4,4,4-trifluorobutylamino)benzonitrile
11 (13.71 g, 50.18 mmol) in MeOH (250 mL) was flushed with N₂, charged
12 with 10 wt.% palladium on carbon (534 mg, 0.50 mmol) and purged
13 with hydrogen. The reaction mixture was stirred under an atmosphere
14 of hydrogen (balloon) at rt overnight. The reaction mixture was
15 filtered through a pad of Celite and washed with MeOH until the
16 filtrate was colourless. The filtrate was evaporated *in vacuo* to
17 give the crude product as a dark solid (12.6 g). Recrystallization
18 from EtOAc/petroleum ether afforded 2× batches of product as a
19 grey solid (batch 1: 2.56 g; batch 2: 2.17 g). The filtrate from
20 the recrystallization was evaporated under reduced pressure, and
21 purified (SiO₂, 40-70% EtOAc in petroleum ether) to afford a
22 purplish dark grey solid (6.02 g). Combined yield: 10.75 g, 88%.
23
24
25
26
27
28
29
30
31
32
33
34
35
36
37
38
39
40 ¹H NMR (600 MHz, CDCl₃) δ 7.19 (dd, $J = 8.3, 1.8$ Hz, 1H), 7.02 (d,
41 $J = 1.8$ Hz, 1H), 6.60 (d, $J = 8.3$ Hz, 1H), 3.27 (t, $J = 7.1$ Hz,
42 2H), 2.24 (tdt, $J = 16.0, 10.7, 5.7$ Hz, 2H), 1.95 (p, $J = 7.2$ Hz,
43 2H). LCMS (ESI+) m/z 244.3 [M+H]⁺ at 3.28 min.
44
45
46
47
48

49 **[5-Cyano-1-(4,4,4-trifluorobutyl)benzimidazol-2-yl]methyl acetate**

50 Acetoxyacetyl chloride (2.21 mL, 20.56 mmol) was added dropwise
51 via a syringe to a stirred and cooled (0 °C) solution of 3-amino-4-
52
53
54
55
56
57
58
59
60

1
2
3 (4,4,4-trifluorobutylamino)benzotrile (5.0 g, 20.56 mmol) and
4
5 NEt₃ (5.73 mL, 41.11 mmol) in anhydrous CH₂Cl₂ (75 mL). The reaction
6
7 mixture was allowed to attain rt and stirred for 2 h. The volatiles
8
9 were removed *in vacuo*, and the residue was dissolved in acetic
10
11 acid (30 mL) and stirred at 80 °C for 16 h. The volatiles were
12
13 removed under reduced pressure and the residue taken up in CH₂Cl₂
14
15 (200 mL), then washed with saturated solution of Na₂CO₃ (3× 100
16
17 mL), dried (MgSO₄) and the solvent removed under reduced pressure.
18
19 Purification by flash chromatography (SiO₂, 40-80% EtOAc in
20
21 petroleum ether) followed by trituration afforded an off-white
22
23 solid (4.61 g, 69%). ¹H NMR (500 MHz, DMSO-*d*₆) δ 8.27 – 8.15 (m, 1H), 7.89
24
25 (dd, *J* = 8.4, 0.7 Hz, 1H), 7.71 (dd, *J* = 8.4, 1.5 Hz, 1H), 5.37 (s, 2H), 4.40 (t, *J* = 7.7 Hz, 2H), 2.46
26
27 – 2.32 (m, 2H), 2.09 (s, 3H), 2.05 – 1.90 (m, 2H). LCMS (ESI+) *m/z* 326.1 [M+H]⁺ at 3.26 min.

32
33 **2-(Hydroxymethyl)-1-(4,4,4-trifluorobutyl)benzimidazole-5-**
34
35 **carbonitrile (40)**

36
37 A suspension of [5-cyano-1-(4,4,4-trifluorobutyl)benzimidazol-2-
38
39 yl]methyl acetate (7.44 g, 22.87 mmol) and potassium carbonate
40
41 (6.32 g, 45.74 mmol) in MeOH (120mL) was stirred at rt for 1 h.
42
43 The reaction mixture was concentrated *in vacuo*, CH₂Cl₂ (200 mL)
44
45 added, the mixture stirred for 10 min, then filtered, washing with
46
47 CH₂Cl₂ and the filtrate concentrated *in vacuo*. Purification by
48
49 flash chromatography (SiO₂, 0-5% MeOH in CH₂Cl₂) followed by
50
51 trituration with Et₂O afforded a white solid (3.90 g). The Et₂O
52
53 triturate was concentrated *in vacuo* and purified by flash
54
55
56
57
58
59
60

1
2
3 chromatography (SiO₂, 0-5% MeOH in CH₂Cl₂) to afford a second crop
4
5 of product (2.02 g, pink solid). Combined yield: 5.92 g, 91%. ¹H
6
7 NMR (600 MHz, DMSO-*d*₆) δ 8.14 (dd, *J* = 1.5, 0.7 Hz, 1H), 7.84 (dd,
8
9 *J* = 8.4, 0.7 Hz, 1H), 7.66 (dd, *J* = 8.4, 1.5 Hz, 1H), 5.80 – 5.70
10
11 (m, 1H), 4.75 (d, *J* = 5.4 Hz, 2H), 4.40 (t, *J* = 7.6 Hz, 2H), 2.44
12
13 – 2.28 (m, 2H), 2.00 (dq, *J* = 12.0, 7.8 Hz, 2H).

14
15
16 LCMS (ESI+) *m/z* 284.2 [M+H]⁺ at 2.06 min.

17
18
19
20
21 ***tert*-Butyl N-[[2-(hydroxymethyl)-1-(4,4,4-**
22
23 **trifluorobutyl)benzimidazol-5-yl]methyl]carbamate**

24
25
26 Palladium hydroxide on activated carbon (20 wt.%; 773 mg, 5.51mmol)
27
28 was added to a solution of 2-(hydroxymethyl)-1-(4,4,4-
29
30 trifluorobutyl)benzimidazole-5-carbonitrile (4.33 g, 15.29mmol)
31
32 in MeOH (150 mL) and THF (77 mL). The reaction was purged with H₂,
33
34 hydrogen chloride (0.4M solution in water; 37 mL, 15.26 mmol) added
35
36 and stirred under an atmosphere of hydrogen via a balloon at rt
37
38 overnight. The reaction was filtered through a pad of Celite,
39
40 washing with MeOH (3× 30 mL), and the filtrate concentrated *in*
41
42 *vacuo*. The residue was diluted with water (50 mL) and basified to
43
44 pH ≈ 9.5 with saturated aqueous Na₂CO₃ solution. The resulting
45
46 suspension was then concentrated to dryness under reduced
47
48 pressure. The residue was suspended in MeCN/Et₂O (1:1, 2× 50 mL)
49
50 and filtered. The precipitate was washed with EtOH (6× 50 mL), and
51
52 the solvent removed under reduced pressure to afford a white solid
53
54
55
56
57
58
59
60

(4 g). The precipitate was washed further with EtOH (3× 30 mL) and the solvent removed under reduced pressure. The filtrate from the MeCN/Et₂O wash was also concentrated under reduced pressure, and the combined residues purified by flash chromatography [SiO₂, eluting with CH₂Cl₂:MeOH:NH₃ (100:0:0 to 90:10:2)] afforded a further 380 mg of off-white solid. The combined material (~4.38 g) was taken to the next step without further purification.

Di-tert-butyl dicarbonate (3.26 g, 14.92 mmol) was added portionwise to a solution of crude 5-(aminomethyl)-1-(4,4,4-trifluorobutyl)benzimidazol-2-yl]methanol (4.38 g, 15.25 mmol) and N,N-diisopropylethylamine (4.82 mL, 27.67 mmol) in CH₂Cl₂ (150 mL) under N₂ and the reaction stirred at rt for 3 h. The volatiles were removed under reduced pressure, the crude suspended in petroleum ether:EtOAc (~8:2; 50 mL) and filtered. The precipitate was washed with petroleum ether:EtOAc (~8:2; 3× 50 mL), and the filtrate discarded. The precipitate was washed with water H₂O (2× 50 mL) and dried in a vacuum oven. The solid was then triturated with MeOH (30 mL), and dried to afford a white solid (4.93 g, 83%).

¹H NMR (500 MHz, DMSO-*d*₆) δ 7.52 (d, *J* = 8.4 Hz, 1H), 7.44 (s, 1H), 7.39-7.32 (m, 1H), 7.14 (d, *J* = 8.3 Hz, 1H), 5.60 (t, *J* = 5.7 Hz, 1H), 4.70 (d, *J* = 5.5 Hz, 2H), 4.33 (t, *J* = 7.4 Hz, 2H), 4.20 (d, *J* = 6.2 Hz, 2H), 2.43 - 2.26 (m, 3H), 2.00 (p, *J* = 7.6 Hz, 2H), 1.39 (s, 9H). LCMS (ESI+) *m/z* 388.1 [M+H]⁺ at 0.57 min.

1
2
3 **tert-Butyl N-[[2-(chloromethyl)-1-(4,4,4-**
4
5 **trifluorobutyl)benzimidazol-5-yl]methyl]carbamate (41)**
6

7
8 Methanesulfonyl chloride (193 μ L, 2.50mmol) was added dropwise via
9
10 syringe to a cooled (0 °C) solution of tert-butyl N-[[2-
11
12 (hydroxymethyl)-1-(4,4,4-trifluorobutyl)benzimidazol-5-
13
14 yl]methyl]carbamate (0.88 g, 2.27 mmol) and N,N-
15
16 diisopropylethylamine (1.19 mL, 6.81mmol) in THF (15 mL). The
17
18 reaction mixture was allowed to warm to rt and stirred overnight.
19
20 The reaction was quenched with water (10 mL) and the volatiles
21
22 removed under reduced pressure. The residue was diluted with water
23
24 (25 mL) and extracted with EtOAc (2 \times 25 mL). The combined organic
25
26 extracts were washed with saturated citric acid solution, then
27
28 saturated aqueous NaHCO₃ solution, dried (MgSO₄) and the solvent
29
30 removed under reduced pressure to afford a light orange oil (880
31
32 mg, 96%) which was used without further purification. ¹H NMR (500
33
34 MHz, DMSO-*d*₆) δ 7.58 (d, *J* = 8.3 Hz, 1H), 7.48 (s, 1H), 7.38 (t, *J*
35
36 = 6.4 Hz, 1H), 7.21 (d, *J* = 8.3 Hz, 1H), 5.06 (s, 2H), 4.36 (t, *J*
37
38 = 7.6 Hz, 2H), 4.21 (d, *J* = 6.3 Hz, 2H), 2.38 (ddt, *J* = 14.8, 8.6,
39
40 3.2 Hz, 2H), 2.06 - 1.98 (m, 2H), 1.39 (s, 9H). LCMS (ESI+) *m/z*
41
42 406.0 [M+H]⁺ at 3.74 min. HRMS (ESI): *m/z* [M+H]⁺ calcd. for
43
44 C₁₈H₂₄ClF₃N₃O₂ 406.1504, found 406.1503.
45
46
47
48
49

50
51 **6' Fluoro-1',2'-dihydrospiro[cyclopropane-1,3'-indole]-2'-one**
52
53 **(43)**
54
55
56
57
58
59
60

1
2
3 A solution of 6-fluoroindolin-2-one (1.63 g, 10.79 mmol) and
4 diisopropylamine (3.17 mL, 22.65 mmol) in anhydrous
5 tetrahydrofuran (18 mL) under N₂ was cooled down at -40 °C using
6 a dry ice/acetonitrile bath. *n*-Butyllithium solution (2.5 M in
7 hexanes; 17.26 mL, 43.14 mmol) was added dropwise via syringe
8 over 15 min. Upon complete addition, the dry ice/acetonitrile
9 bath was changed for an ice bath and the reaction allowed to
10 warm to 0 °C. A solution of 1,2-dibromoethane (2.79 mL, 32.35
11 mmol) in THF (7 mL) was then added dropwise and the reaction
12 mixture stirred at rt overnight. The reaction was quenched with
13 saturated aq. NH₄Cl (60 mL) and diluted with EtOAc (100 mL) and
14 the phases separated. The aqueous layer was extracted with EtOAc
15 (50 mL) and the combined organic layers with brine (2× 75 mL),
16 dried (MgSO₄) and the solvent removed under reduced pressure.
17 The crude was purified by flash chromatography (SiO₂, 0-100%
18 EtOAc in petroleum ether) to afford an orange solid (902 mg,
19 47%). ¹H NMR (500 MHz, CDCl₃) δ 8.49 (s, 1H), 6.79 - 6.67 (m, 3H),
20 1.76 (q, J = 3.9 Hz, 2H), 1.53 (q, J = 4.2 Hz, 2H). LCMS (ESI+)
21 *m/z* 178.2 [M+H]⁺ at 1.31 min.

22 **tert-butyl**

23 **N-([2-((6'-fluoro-2'-oxo-1',2'-dihydrospiro[cyclopropane-1,3'-indole]**
24 **-1'-yl)methyl)-1-(4,4,4-trifluorobutyl)-1H-1,3-benzodiazol-5-yl]methy**
25 **l) carbamate (44)**

1
2
3 Sodium hydride (60% dispersion in mineral oil; 0.11 mL, 2.75 mmol)
4
5 was added in one portion to cooled (0 °C) solution of 6'-fluoro-
6
7 1,2-spiro[cyclopropane-1,3'-indole]-2'-one (487 mg, 2.75 mmol) in
8
9 DMF (10 mL) under nitrogen. The reaction was allowed to attain rt
10
11 and stirred for 1 h. A solution of crude N-[[2-(chloromethyl)-1-
12
13 (4,4,4-trifluorobutyl)-1H-1,3-benzodiazol-5-yl]methyl]carbamate
14
15 (1.01 g, 2.48 mmol) in DMF (4 mL) was then added by dropwise
16
17 addition over 5 minutes, and the reaction mixture stirred at rt
18
19 for 16 h. The reaction was quenched with water (100 mL) and
20
21 extracted with EtOAc (3× 75 mL). The combined organics were washed
22
23 with water (100 mL), brine (120 mL), then dried (MgSO₄) and
24
25 evaporated under reduced pressure. The crude oil was purified by
26
27 flash chromatography (SiO₂, 0-100% EtOAc in petroleum ether)
28
29 followed by trituration with petroleum ether/EtOAc (4:1; 10 mL) to
30
31 afford a yellow solid (1030 mg, 75%). ¹H NMR (500 MHz, CDCl₃) δ 7.74
32
33 - 7.70 (m, 1H), 7.34 (dd, J = 9.1, 2.1 Hz, 1H), 6.77 - 6.66 (m,
34
35 2H), 5.30 - 5.26 (m, 2H), 4.91 (s, 1H), 4.45 (d, 2H), 4.33 (t, J
36
37 = 7.9 Hz, 2H), 2.20 - 2.06 (m, 2H), 1.91 - 1.81 (m, 2H), 1.81 -
38
39 1.72 (m, 2H), 1.63 (d, J = 1.0 Hz, 1H), 1.59 - 1.53 (m, 2H), 1.48
40
41 (s, 9H). ¹³C NMR (100 MHz, CDCl₃) δ 177.1, 162.3 (d, J_{CF} = 245 Hz),
42
43 148.4, 143.1 (d, J_{CF} = 12 Hz), 142.6, 134.5, 133.8, 127.0, 125.3,
44
45 123.5, 119.1 (d, J_{CF} = 9 Hz), 118.96, 109.6, 109.1 (d, J_{CF} = 23Hz),
46
47 99.6 (d, J_{CF} = 30 Hz), 77.2, 42.7, 38.2, 31.1 (q, J_{CF} = 28 Hz),
48
49 26.7, 22.7, 22.6, 22.58, 19.6. LCMS m/z [M+ H]⁺ 547.2 at 4.55 min.
50
51
52
53
54
55
56
57
58
59
60

1
2
3 **1' - ([5- (Aminomethyl) -1- (4,4,4-trifluorobutyl) -1H-1,3-**
4
5 **benzodiazol-2-yl]methyl) -6' fluoro-1',2' -**
6
7 **dihydrospiro[cyclopropane-1,3'-indole]-2'-one (20)**

8
9
10 To a solution of tert-butyl N-[(2-[(6'-fluoro-2'-oxo-1',2'-
11 dihydro[spirocyclopropane-1,3'-indole]-1'-ylmethyl]-1-(4,4,4-
12 trifluorobutyl)-1H-1,3-benzodiazyl)methyl]carbamate (1030 mg,
13
14 1.88 mmol) in CH₂Cl₂ (3.5 mL) under nitrogen was added hydrogen
15
16 chloride solution (2 M in Et₂O; 12.54 mL, 25.08 mmol). A pink/white
17
18 solid precipitate formed almost immediately, and the mixture was
19
20 stirred at rt for 6 h. The reaction mixture was concentrated under
21
22 reduced pressure at ambient temperature and azeotrope with CH₂Cl₂
23
24 (3× 20 mL) to avoid HCl concentration. The crude product was
25
26 sonicated and triturated with Et₂O (2× 15 mL, then 4× 10 mL). The
27
28 mixture was filtered, washing with (Et₂O (3× 10 mL) and dried in a
29
30 vacuum oven to give the crude HCl salt of the desired product as
31
32 an off-white solid (851 mg, 89% crude yield).

33
34
35 The crude HCl salt was partitioned between EtOAc (80 mL) and
36
37 saturated aqueous NaHCO₃ solution (80 mL). The organic phase was
38
39 separated, and the aqueous layer extracted with EtOAc (3× 30 mL).
40
41 The organics were combined, dried (MgSO₄), and concentrated under
42
43 reduced pressure. The residue was triturated with Et₂O (15 mL),
44
45 then purified by flash chromatography on [SiO₂, 0-50%
46
47 CH₂Cl₂:MeOH:NH₃ (9:1:0.2) in CH₂Cl₂] to afford the free base as a
48
49 white solid (539 mg, 63%). ¹H NMR (400 MHz, DMSO-*d*₆) δ 7.58 (d, *J* =

1
2
3 1.5Hz, 1H), 7.54 (d, $J = 8.3$ Hz, 1H), 7.24 (dd, $J = 8.4$, 1.6Hz,
4
5 1H), 7.17 (dd, $J = 9.6$, 2.4Hz, 1H), 7.06 (dd, $J = 8.3$, 5.4Hz,
6
7 1H), 6.81 (ddd, $J = 10.5$, 8.2, 2.4Hz, 1H), 5.29 (s, 2H), 4.36 (t,
8
9 $J = 7.7$ Hz, 2H), 3.79 (s, 2H), 2.39-2.26 (m, , 2H), 1.88-1.80 (m,
10
11 , 2H), 1.67 (q, $J = 4.1$, 3.4 Hz, 2H), 1.59 (q, $J = 4.5$, 3.9 Hz,
12
13 2H). ^{13}C NMR (100 MHz, DMSO- d_6) δ 176.3, 161.4 (d, $J_{\text{CF}} = 239.7$ Hz),
14
15 148.8, 143.65 (d, $J_{\text{CF}} = 12.2$ Hz), 142.0, 137.7, 133.9, 127.2 (q,
16
17 $J_{\text{CF}} = 276.7$ Hz), 125.6 (d, $J_{\text{CF}} = 2.4$ Hz), 122.5, 120.2 (d, $J_{\text{CF}} =$
18
19 9.7 Hz), 117.4, 109.8, , 108.0 (d, $J_{\text{CF}} = 22.5$ Hz), 98.2 (d, $J =$
20
21 28.2 Hz), 45.7, 41.9, 37.2, 30.1 (q, $J_{\text{CF}} = 28.4$ Hz), 26.3, 22.2,
22
23 19.9. HRMS (ESI): m/z $[\text{M}+\text{H}]^+$ calcd. for $\text{C}_{23}\text{H}_{23}\text{N}_4\text{OF}_4$: 447.1808,
24
25 found: 447.1816. LCMS m/z $[\text{M}+ \text{H}]^+$ 447.3 at 0.58 min.

26
27
28
29
30 **1'-([5-(Aminomethyl)-1-(4,4,4-trifluorobutyl)-1H-1,3-**
31
32 **benzodiazol-2-yl)methyl)-6' fluoro-1',2'-**
33
34 **dihydrospiro[cyclopropane-1,3'-indole]-2'-one hydrochloride**
35
36 **(20 ·HCl)**

37
38
39 HCl (2.0 M in Et_2O ; 0.6 mL, 1.21 mmol) was added dropwise to a
40
41 solution of 1'-([5-(aminomethyl)-1-(4,4,4-trifluorobutyl)-1H-1,3-
42
43 benzodiazol-2-yl)methyl)-6' fluoro-1',2'-
44
45 dihydrospiro[cyclopropane-1,3'-indole]-2'-one (539 mg, 1.21
46
47 mmol) in CH_2Cl_2 (10 mL) and the reaction mixture stirred for 30
48
49 min. The solvent was then evaporated under vacuum. The residue was
50
51 dissolved in MeOH (20 mL), concentrated under vacuum at rt, and
52
53 dried further in a vacuum oven at 40 °C, affording the
54
55
56
57
58
59
60

1
2
3 hydrochloride salt as a white solid (480 mg, 81%). ¹H NMR (600
4 MHz, DMSO-*d*₆) δ 8.39 (br. s, 3H), 7.75 (d, *J* = 1.5 Hz, 1H), 7.68
5
6 (d, *J* = 8.3 Hz, 1H), 7.40 (dd, *J* = 8.4, 1.6 Hz, 1H), 7.14 (dd, *J*
7
8 = 9.6, 2.4 Hz, 1H), 7.08 (dd, *J* = 8.3, 5.4 Hz, 1H), 6.82 (ddd, *J*
9
10 = 10.3, 8.3, 2.4 Hz, 1H), 5.33 (s, 2H), 4.40 (t, *J* = 7.7 Hz, 2H),
11
12 2.40 - 2.27 (m, 2H), 1.88-1.83 (m, 2H), 1.69 (q, *J* = 3.9 Hz, 2H),
13
14 1.58 (q, *J* = 3.8 Hz, 2H)). ¹³C NMR (150 MHz, DMSO-*d*₆) δ 176.35,
15
16 161.4 (d, *J* = 240 Hz), 149.8, 143.6 (d, *J* = 12 Hz), 141.8, 135.1,
17
18 127.2 (q, *J* = 276 Hz), 127.8, 125.65 (d, *J* = 2 Hz), 123.8, 120.3
19
20 (d, *J* = 10 Hz), 120.0, 110.4, 108.05 (d, *J* = 22.5 Hz), 98.1 (d, *J*
21
22 = 28 Hz), 42.6, 42.0, 37.2, 30.0 (q, *J* = 28 Hz), 26.35, 22.2, 18.9.
23
24 HRMS (ESI): *m/z* [M+H]⁺ calcd. for C₂₃H₂₃N₄O₄F₄: 447.1808, found:
25
26 447.1805.
27
28
29
30
31
32
33
34

35 **RSV fusion assay**

36
37
38 The inhibition of RSV F protein mediated cell-cell fusion was
39
40 investigated in an *in vitro* RSV F protein cell-cell fusion assay
41
42 based on the method of Branigan *et al.*²⁴ Briefly, human embryonic
43
44 kidney 293T cells (ATCC, CRL-11268) were co-transfected with an
45
46 expression plasmid encoding the RSV F protein from the RSV A2
47
48 strain (pCDNA3.1-A2-F; codon optimised F protein sequence from RSV
49
50 strain A2 was synthesised (GeneArt) and subcloned into pCDNA3.1(+)
51
52 (Invitrogen, V79020) and a reporter plasmid containing the
53
54
55
56
57
58
59
60

1
2
3 luciferase gene under the control of a GAL4 responsive promoter
4 (pFR-Luc, Stratagene 219050). A second set of 293T cells were
5
6 (pFR-Luc, Stratagene 219050). A second set of 293T cells were
7
8 transfected with an expression plasmid encoding a transcriptional
9
10 transactivator fusion protein consisting of the GAL4 DNA binding
11
12 domain fused to the activation domain of NF- κ B (pCDNA3.1 GAL4/NF κ B:
13
14 GAL4-NF- κ B sequence was synthesised (Genscript) and subcloned into
15
16 pCDNA3.1(+) (Invitrogen, V79020). After 24 h, the 2 cell
17
18 populations were mixed in the presence of 3-fold serial dilutions
19
20 of test compound and the RSV F protein-mediated fusion between the
21
22 2 cell populations measured by quantifying the luciferase activity
23
24 induced by the co-localisation of the GAL4-NF- κ B transactivator
25
26 fusion protein and the GAL 4 responsive luciferase reporter
27
28 expression plasmid after 24 h.
29
30
31
32
33
34

35 **Plaque Reduction Assay:**

36
37 The inhibition of RSV infection of cells was investigated in an *in*
38
39 *vitro* RSV plaque assay. African green monkey kidney (Vero) or HepG2
40
41 cell cultures were infected with the RSV strain A2 or low passage
42
43 clinical strains of RSV for 48 h in the presence of a range of
44
45 test compound concentrations (0.01 nM - 100 μ M) prior to detection
46
47 of distinct foci of infection (plaques) by immunostaining.
48
49
50

51 **Cell Cytotoxicity Assay:**

52
53 Cell cytotoxicity was assessed in parallel to plaque reduction
54
55 assays. African green monkey kidney (Vero) cells, HepG2 or Hep2
56
57
58
59
60

1
2
3 cells were cultured in the presence of a range of test compound
4 concentrations (0.01 nM - 100 μ M) prior to measurement of cell
5 viability by the addition of MTT (3-(4,5-dimethylthiazol-2-yl)-
6 2,5-diphenyltetrazolium bromide), CellTox green
7 (Promega) or CellTitre-Glo (Promega).
8
9
10
11
12
13
14
15
16

17 **Inhibition of RSV in primary human airway epithelial cells**

18
19 The inhibition of RSV was investigated in an *in*
20 *vitro* primary HAE cell infectivity model²⁵. Briefly, HAE cells were
21 differentiated on Type IV collagen coated trans-well plate inserts
22 for 61 days. Differentiated HAE cell cultures (n=3) were pre-
23 incubated with compound (10 nM) for 2 hours, prior to apical
24 inoculation with 4×10^5 plaque forming units (pfu) recombinant
25 luciferase-expressing RSV (lucRSV). Samples of lucRSV shed by the
26 infected HAE cells were obtained daily, for eight consecutive days,
27 by washing the HAE apical cell surface for 2 hours. Analysis of
28 RSV yield in the HAE apical samples was conducted by infecting
29 human lung epithelial A549 cells and determining the luciferase
30 activity 24 hours post infection (pi). On day 8 pi, the HAE cells
31 were fixed and stained with H&E for histological examination.
32
33
34
35
36
37
38
39
40
41
42
43
44
45
46
47
48
49
50

51 **Animal experiments**

52
53 All animal experimentation was covered under the UK Animals
54 (Scientific Procedures) Act (1986) and EU directive 86/609/EEC.
55
56
57
58
59
60

1
2
3 All such work was monitored by regular inspections of procedures
4 and facilities by the on-site Veterinarian and UK Home Office
5 inspectors.
6
7
8
9

11 ***in vivo* Pharmacokinetics**

12
13
14 The pharmacokinetics of the compounds were studied *in vivo* in male
15 Sprague Dawley rats at doses of 1 mg/kg (IV) and 10 mg/kg (PO).
16
17 Sprague Dawley rats were treated with experimental compounds via
18 intravenous and oral administration. Three animals for each route
19 of administration were used with serial blood sampling at ten time
20 points post dosing of compound.
21
22
23
24
25
26
27

28 An intravenous bolus was administered at a dose of 1 mg/kg and at
29 a concentration of 1 mg/ml in 40:60 dimethyl acetamide/saline (0.9%
30 w/v saline). Animals were weighed and used if between 200-250 g.
31
32 Serial blood samples were collected at 0.02, 0.08, 0.25, 0.50, 1,
33 2, 4, 6, 8 and 24 h post dosing. Animals were observed for any
34 overt clinical signs or symptoms. Blood samples were delivered
35 into an anticoagulant (sodium heparin) and centrifuged at 4 °C.
36
37 Plasma samples were subsequently stored frozen at less than -20 °C
38 prior to analysis.
39
40
41
42
43
44
45
46
47

48 Following protein precipitation with acetonitrile, samples were
49 analysed with tandem liquid chromatography/mass spectrometry using
50 electrospray ionisation. A full matrix curve with internal
51 standards was employed and PK parameters were calculated.
52
53
54
55
56
57
58
59
60

1
2
3 In a similar manner, oral administration was performed by gavage
4
5 at doses of 5 or 10 mg/kg at a concentration of 5 mg/mL in 1%
6
7 methyl cellulose (Sigma M7140), 0.1% Tween 80 in water. Serial
8
9 samples were taken as described above.
10

11
12 Acclimatized male CD-1 mice were group housed in a temperature
13
14 and light controlled facility on a 12-hour light/dark cycle with
15
16 food and water available *ad libitum*. Mice included in the study
17
18 were individually housed until completion. All animals were
19
20 subjected to health monitoring in accordance with the above
21
22 guidelines by the onsite Home Office registered veterinarian.
23
24

25
26 Animals were anaesthetized and terminal blood samples were
27
28 collected by cardiac puncture. Samples were transferred into
29
30 heparinized polypropylene tubes on wet ice and centrifuged at 4°C
31
32 within 15 minutes, to yield plasma which was snap-frozen and stored
33
34 at -20°C. Sampling time points were 2, 5, 15 min. and 1, 2, 4, 8,
35
36 12, 24 hours for the *in vitro* arm and 5, 15, 30 min, 1, 1.5, 2, 4,
37
38 6, 8, 12 and 24 h for the *oral* arm. Samples were analyzed by
39
40 UHPLC-TOF that comprised an Agilent 1290 HPLC pump with an Agilent
41
42 1290 autosampler, coupled with an Agilent 6550 quadrupole-TOF mass
43
44 spectrometer. The system was controlled by MassHunter software
45
46 vB.05.01
47
48
49

50
51 Six male Beagle dogs (non-naive, 12-13 kg) were housed in pairs
52
53 and acclimatized in a temperature and light controlled on a 12-
54
55 hour light/dark cycle, with food offered each morning and water
56
57
58
59
60

1
2
3 available ad libitum. On dosing days dogs were fed 2 hours after
4
5 dose administration with water available *ad libitum*. Prior to
6
7 commencement of each dosing session each dog was examined by a
8
9 qualified Veterinary Surgeon for suitability for the study.

10
11 Serial blood samples were collected into heparinized polypropylene
12
13 tubes and immediately centrifuged at 4°C for 10 min at 3,000 G to
14
15 yield plasma which was snap-frozen and stored at -20° C. Sampling
16
17 times were 2, 5, 15 min. and 1, 2, 4, 8, 12, 24 h. for the *in vitro*
18
19 arm and 15, 30 min., 1, 1.5, 2, 4, 6, 8, 12 and 24 h for the *oral*
20
21
22 arm.
23
24

25
26 Samples were analyzed by UHPLC-TOF that comprised an Agilent 1290
27
28 HPLC pump with an Agilent 1290 autosampler, coupled with an Agilent
29
30 6550 quadrupole-TOF mass spectrometer. The system was controlled
31
32 by MassHunter software vB.05.01
33
34
35
36

37 **Efficacy in a Balb/C Mouse Model of RSV**

38
39 Briefly, Balb/C mice (6 per treatment group, 7-8-week-old females)
40
41 received two PO doses of compound (0, 1, 10 or 50 mg/mL) 2 hours
42
43 pre- and 24 hours post intranasal inoculation with 5×10^6 pfu of
44
45 RSV strain A2. Animals were euthanized 5 days post RSV inoculation
46
47 and lung homogenates prepared. RSV titres in lung homogenates were
48
49 evaluated by plaque assay on Vero cells.
50
51
52
53
54

55 **ASSOCIATED CONTENT**

Supporting Information

Procedures for *in vitro* ADME assays, virology data, synthetic procedures. Synthetic procedures and characterization of all other compounds and key intermediates, molecular strings. This material is available free of charge via the Internet at <http://pubs.acs.org>.

Crystallographic data and procedures.

For PDB code 7KQD (RSV Fusion protein with compound **20** bound), the authors will release the atomic coordinates and experimental data upon article publication.

AUTHOR INFORMATION

Corresponding Author

*Phone: +44 (0) 1740 625250. E-mail: scockerill@reviral.co.uk

ORCID

G. Stuart Cockerill: 0000-0002-6340-0808

James A. D. Good: 0000-0003-2377-030X

Professor Simon E. Ward: 0000-0002-8745-8377

Present Addresses

1
2
3 †Richard Angell. Head, Drug Discovery Group. Translational
4
5 Research Office, School of Pharmacy, University College London, 9-
6
7 39 Brunswick Square, London. WC1N 1AX. UK
8
9

10
11 †† Ian Fraser. CRL, Chesterford Research Park, Saffron Walden,
12
13 Essex. CB10 1XL. UK
14

15 ‡ James Lumley, Molecular Design, Data and Computational Sciences,
16
17 GlaxoSmithKline, Medicines Research Centre, Gunnels Wood Road,
18
19 Stevenage, Hertfordshire. SG1 2FX. UK
20
21

22
23 ‡‡ Sara M. Johnson. Office of Research, University of Michigan
24
25 Medical School, Ann Arbor, MI.
26

27 # Claire Scott. Covance, Springfield House, Hyde Street, Leeds,
28
29 LS2 9LH, UK.
30

31 **Notes**

32
33

34 Unless stated, the authors declare no competing financial
35
36 interests. GSC, AB, JADG, RH, EL, NM, ET and KP are employees
37
38 and shareholders in Reviral Ltd. RMA IF, JL, CS are
39
40 shareholders in Reviral Ltd. MEP has received research grants
41
42 from NIH (#AI112524; AI095684; AI093848), from the Cystic
43
44 Fibrosis Foundation, from Pfizer and from Janssen, and fees for
45
46 participation in an advisory board from ReViral and lectures
47
48 from Pfizer. D.T. reports receiving personal fees from ReViral
49
50 outside the submitted work.
51
52
53
54
55
56
57
58
59
60

1
2
3 Funding of the work described herein was provided initially by a
4 self-funding initiative of the founders of Reviral Ltd.
5
6 Subsequently the project was progressed via a Wellcome Trust
7
8 Seeding Drug Discovery Award (WT100544) with Professor Simon Ward,
9
10 then of the University of Sussex as co-applicant. Subsequent
11
12 funding was provided by Reviral Ltd., supported both from "angel"
13
14 investor sources and blue-chip venture capital.
15
16
17
18
19

20 ACKNOWLEDGMENT

21
22 Authors contributed to the writing of the manuscript. In
23
24 addition, thanks are to Desmond O'Connor and Mohammad Avalijeh
25
26 of Pharmidex UK for support to pharmacokinetic studies. To Alan
27
28 Kenwright, Jackie Mosely and Juan Aquilar-Malavia of Durham
29
30 University analytical department for NMR and MS support.
31
32
33
34
35
36

37 ABBREVIATIONS

38
39 A_2B , B_2A , direction of compound permeability; BID, twice daily
40
41 dosing; CHF, chronic heart failure; Cl_{int} , intrinsic clearance;
42
43 DIPEA, *N,N*-diisopropylethylamine ERD, enhanced respiratory
44
45 disease; f_u , fraction unbound; $\Delta clogD_{7.4}$, change in calculated log
46
47 D at pH 7.4; $\Delta tPSA$, change in total polar surface area; ERD,
48
49 enhanced respiratory disease; F protein, fusion protein; GLP, good
50
51 laboratory practice; G protein, glycoprotein; HAE, human airway
52
53 epithelial; HBSS, Hanks balanced salt solution; HCT, hematopoietic
54
55
56
57
58
59
60

1
2
3 cell transplant; Hep2, human epithelial type 2 cells; lucRSV,
4 luciferase expressing respiratory syncytial virus; LO, lead
5 optimization; mAb, monoclonal antibody; LRTI, lower respiratory
6 tract infection; M protein, matrix protein; MTT, 3-(4,5-
7 dimethylthiazol-2-yl)-2,5-diphenyltetrazolium bromide; NOAEL, no
8 observed adverse event level; N protein, nucleoprotein; P_{app} ,
9 apparent permeability; P protein, phosphoprotein; pi, post
10 infection; PFU, plaque forming units; PRA, plaque reduction assay;
11 RSV, respiratory syncytial virus; RSV A2, respiratory syncytial
12 virus A2 strain; SAD, single ascending dose; t_{max} , time to maximum
13 absorption; URTI, upper respiratory tract infection;

24 REFERENCES

- 25
26
27
28
29
30 1. Falsey, A. R.; Hennessey, P. A.; Formica, M. A.; Cox, C.;
- 31 Walsh, E. E. Respiratory syncytial virus infection in the
32 elderly and high-risk adults. *N. Engl. J. Med.* 2005, 352,
33 1749-1759.
- 34
35
36
37
38
39 2. (a) Shi, T.; McAllister, D. A.; O'Brien, K. L.; Simoes, E. A.
- 40 F.; Madhi, S. A.; Gessner, B. D.; Polack, F. P.; Balsells, E.;
- 41 Acacio, S.; Aguayo, C.; Alassani, I.; Ali, A.; Antonio, M.;
- 42 Awasthi, S.; Awori, J. O.; Azziz-Baumgartner, E.; Baggett, H.
- 43 C.; Baillie, V. L.; Balmaseda, A.; Barahona, A.; Basnet, S.;
- 44 Bassat, Q.; Basualdo, W.; Bigogo, G.; Bont, L.; Breiman, R.
- 45 F.; Brooks, W. A.; Broor, S.; Bruce, N.; Bruden, D.; Buchy,
- 46 P.; Campbell, S.; Carosone-Link, P.; Chadha, M.; Chipeta, J.;
- 47
48
49
50
51
52
53
54
55
56
57
58
59
60

1
2
3 Chou, M.; Clara, W.; Cohen, C.; de Cuellar, E.; Dang, D.-A.;
4
5 Dash-yandag, B.; Deloria-Knoll, M.; Dherani, M.; Eap, T.;
6
7 Ebruke, B. E.; Echavarria, M.; de Freitas Lázaro Emediato, C.
8
9 C.; Fasce, R. A.; Feikin, D. R.; Feng, L.; Gentile, A.;
10
11 Gordon, A.; Goswami, D.; Goyet, S.; Groome, M.; Halasa, N.;
12
13 Hirve, S.; Homaira, N.; Howie, S. R. C.; Jara, J.; Jroundi,
14
15 I.; Kartasasmita, C. B.; Khuri-Bulos, N.; Kotloff, K. L.;
16
17 Krishnan, A.; Libster, R.; Lopez, O.; Lucero, M. G.; Lucion,
18
19 F.; Lupisan, S. P.; Marcone, D. N.; McCracken, J. P.; Mejia,
20
21 M.; Moisi, J. C.; Montgomery, J. M.; Moore, D. P.; Moraleda,
22
23 C.; Moyes, J.; Munywoki, P.; Mutyara, K.; Nicol, M. P.; Nokes,
24
25 D. J.; Nymadawa, P.; da Costa Oliveira, M. T.; Oshitani, H.;
26
27 Pandey, N.; Paranhos-Baccalà, G.; Phillips, L. N.; Picot, V.
28
29 S.; Rahman, M.; Rakoto-Andrianarivelo, M.; Rasmussen, Z. A.;
30
31 Rath, B. A.; Robinson, A.; Romero, C.; Russomando, G.; Salimi,
32
33 V.; Sawatwong, P.; Scheltema, N.; Schweiger, B.; Scott, J. A.
34
35 G.; Seidenberg, P.; Shen, K.; Singleton, R.; Sotomayor, V.;
36
37 Strand, T. A.; Sutanto, A.; Sylla, M.; Tapia, M. D.;
38
39 Thamthitawat, S.; Thomas, E. D.; Tokarz, R.; Turner, C.;
40
41 Venter, M.; Waicharoen, S.; Wang, J.; Watthanaworawit, W.;
42
43 Yoshida, L.-M.; Yu, H.; Zar, H. J.; Campbell, H.; Nair, H.
44
45
46
47
48
49
50
51 Global, regional, and national disease burden estimates of
52
53 acute lower respiratory infections due to respiratory
54
55 syncytial virus in young children in 2015: a systematic review
56
57
58
59
60

- 1
2
3 and modelling study. *The Lancet* **2017**, 390, 946-958. (b)
4
5 Feltes, T. F.; Sondheimer, H. M. Palivizumab and the
6
7 prevention of respiratory syncytial virus illness in pediatric
8
9 patients with congenital heart disease. *Expert Opin. Biol.*
10
11 *Ther.* 2007, 7(9), 1471-1480.
12
13
14 3. Zhou, H.; Thompson, W. W.; Viboud, C. G.; Ringholz, C. M.;
15
16 Cheng, P.-Y.; Steiner, C.; Abedi, G. R.; Anderson, L. J.;
17
18 Brammer, L.; Shay, D. K. Hospitalizations associated with
19
20 influenza and respiratory syncytial virus in the United
21
22 States, 1993-2008. *Clin. Infect. Dis.* **2012**, 54, 1427-1436.
23
24
25 4. Pérez-Yarza, E. G. M., A.; Lažaro, P.; Mejías, A.; Ramilo, O. The
26
27 association between respiratory syncytial virus infection and
28
29 the development of childhood asthma. *Journal of Pediatric*
30
31 *Infectious Disease* **2007**, 26, 733-739.
32
33
34 5. Mac, S.; Sumner, A.; Duchesne-Belanger, S.; Stirling, R.;
35
36 Tunis, M.; and Beate Sander, B. Cost-effectiveness of
37
38 palivizumab for respiratory syncytial virus: a systematic
39
40 review. *Pediatrics* 2019, 143 (5) e20184064; DOI:
41
42 <https://doi.org/10.1542/peds.2018-4064>
43
44
45
46
47 6. (a) Wainwright, C. Acute viral bronchiolitis in children - a
48
49 very common condition with few therapeutic options. *Paediatr.*
50
51 *Respir. Rev.* 2010, 11(1), 39-45. (b) Empey, K. M.; Peebles Jr.,
52
53 R. S.; Kolls, J. K. Pharmacologic advances in the treatment and
54
55
56
57
58
59
60

1
2
3 prevention of respiratory syncytial virus. *Clin. Infect. Dis.*
4
5 2010, 50(9), 1258-1267.
6
7

8
9 7. Collins, P. L. Respiratory Syncytial Virus–Human
10 (Paramyxoviridae). In *Encyclopedia of Virology*, 2nd ed.; G.
11 Allan and G. W. Robert, Ed. Elsevier: Oxford, UK, 1999.
12
13

14
15 8. Hacking, D.; Hull, J. Respiratory syncytial virus--viral
16 biology and the host response. *J. Infect.* **2002**, 45, 18-24.
17
18

19
20 9. Cockerill, G. S.; Good, J. A. D.; Mathews, N. State of the
21 art in respiratory syncytial virus drug discovery and
22 development. *J. Med. Chem.* **2019**, 62, 3206-3227
23
24

25
26 10. Chapman, J.; Cockerill, S. G. Discovery and Development
27 of RSV604, In *Antiviral Drugs: From Basic Discovery Through*
28 *Clinical Trials*. Kazmierski, W. M., Ed. John Wiley & Sons,
29 Inc.: New York, 2011.
30
31

32
33 11. DeVincenzo, J. P.; Whitley, R. J.; Mackman, R. L.;
34 Scaglioni-Weinlich, C.; Harrison, L.; Farrell, E.; McBride, S.;
35 Lambkin-Williams, R.; Jordan, R.; Xin, Y.; Ramanathan, S.;
36 O’Riordan, T.; Lewis, S. A.; Li, X.; Toback, S. L.; Lin, S.-L.;
37 Chien, J. W. Oral GS-5806 Activity in a respiratory syncytial
38 virus challenge study. *New Engl. J. Med.* **2014**, 371, 711-722.
39
40

41
42 12. Martínón-Torres, F.; Rusch, S.; Huntjens, D.; Remmerie, B.;
43 Vingerhoets, J.; McFadyen, K.; Ferrero, F.; Baraldi, E.; Rojo,
44 P.; Epalza, C.; Stevens, M. Pharmacokinetics, safety and
45
46
47
48
49
50
51
52
53
54
55
56
57
58
59
60

1
2
3 antiviral effects of multiple doses of the respiratory syncytial
4 virus fusion protein inhibitor, JNJ-53718678, in infants
5
6 hospitalized with RSV infection: A randomized phase 1b study.
7
8 *Clinical. Infectious. Disease.* **2020**, 71, e594 - e603
9

10
11
12
13
14 13. Zheng, X.; Gao, L.; Wang, L.; Liang, C.; Wang, B.; Liu, Y.;
15 Feng, S.; Zhang, B.; Zhou, M.; Yu, X.; Xiang, K.; Chen, L.; Guo,
16 T.; Shen, H. C.; Zou, G.; Wu, J. Z.; Yun, H. Discovery of
17 ziresovir as a potent, selective, and orally bioavailable
18 respiratory syncytial virus fusion protein inhibitor. *J. Med.*
19 *Chem.* **2019**, 62, 6003-6014.
20
21
22
23
24
25

26
27
28 14. Coakley, E.; Ahmad, A.; Larson, K.; McClure, T.; Lin, K.;
29 Lin, K.; Tenhoor, K.; Eze, K.; Noulin, N.; Horvathova, V.;
30 Murray, B.; Baillet, M.; Mori, J.; Adda, N. LB6. EDP-938, a
31 novel RSV N-inhibitor, administered once or twice daily was safe
32 and demonstrated robust antiviral and clinical efficacy in a
33 healthy volunteer challenge study. *Open Forum Infectious*
34 *Diseases* **2019**, 6, S995.
35
36
37
38
39
40
41
42

43
44 15. Cianci, C.; Yu, K. L.; Combrink, K.; Sin, N.; Pearce,
45 B.; Wang, A.; Civiello, R.; Voss, S.; Luo, G.; Kadow, K.;
46 Genovesi, E. V.; Venables, B.; Gulgeze, H.; Trehan, A.; James,
47 J.; Lamb, L.; Medina, I.; Roach, J.; Yang, Z.; Zadjura, L.;
48 Colonno, R.; Clark, J.; Meanwell, N.; Krystal, M. Orally active
49
50
51
52
53
54
55
56
57
58
59
60

1
2
3 fusion inhibitor of respiratory syncytial virus. *Antimicrob.*
4
5 *Agents Chemother.* **2004**, 48, 413-422.
6
7

8
9 16. Vaudevilles, S.;, Tahri, A.; Hu, L.; Demin, S.; Coymans,
10
11 L.; Vos, A.;

12
13 Kwanten, L.; Van den Berg, J.; Battles, M. B.; McLellan, J. S.;

14
15 Koul, A.; Raboisson, P.; Roymans, D.; Jonckers, T. H. M..

16
17
18 Discovery of 3-({5-chloro-1-[3-(methylsulfonyl)propyl]-1H-indol-2-
19
20 yl)methyl)-1-(2,2,2-trifluoroethyl)-1,3-

21
22 dihydro-2H-imidazo[4,5-c]pyridin-2-one (JNJ-53718678), a potent

23
24 and orally bioavailable fusion inhibitor of respiratory

25
26 syncytial virus. *J. Med. Chem.* 2020, 63, 8046-8058
27
28
29
30
31
32

33 17. Yu, K.-L.; Civiello, R. L.; Combrink, K. D.; Gulgeze, H.

34
35 B.; Sin, N.; Wang, X.; Meanwell, N.; Venables, B. L.; Zhang, Y.;

36
37 Pearce, B. C.; Yin, Z.; Thuring, J. W. Heterocyclic Substituted

38
39 2-Methyl-benzimidazole Antiviral Agents. WO/2002/062290, Nov 21,

40
41
42 2002.
43

44 18. Yu, K.-L.; Wang, X.; Sun, Y.; Cianci, C.; Thuring, J. W.;

45
46 Combrink, K.; Meanwell, N.; Zhang, Y.; Civiello, R. L.

47
48 Substituted 2-Methyl-benzimidazole Respiratory Syncytial Virus

49
50 Antiviral Agents. WO/2003/053344, July 03, 2003.
51
52

53 19. Blade, H.; Carron, E.; Jackson, H.; Lumley, J.; Pilkington,

54
55 C.; Tomkinson, G.; Thomas, A.; Warne, J. Benzimidazole
56
57
58
59
60

1
2
3 Derivatives and their use as Antiviral Agents. WO/2010/103306,
4
5 Sep 17, 2010.
6

7
8 20. Leeson, P. D.; Springthorpe, B. The influence of drug-like
9
10 concepts on decision-making in medicinal chemistry. *Nature*
11
12 *Reviews Drug Discovery* **2007**, 6, 881-890.
13

14
15 21. Edwards, M. P.; Price, D. A. Chapter 23 - Role of
16
17 Physicochemical Properties and Ligand Lipophilicity Efficiency
18
19 in Addressing Drug Safety Risks. In *Annual Reports in Medicinal*
20
21 *Chemistry*, Macor, J. E., Ed. Academic Press, Cambridge, MA:
22
23 2010; Vol. 45, pp 380-391.
24

25
26 22. For a comparable study in the benzimidazolone series of
27
28 fusion inhibitors, see: Yu, K.-L.; Sin, N.; Civiello, R. L.;
29
30 Wang, X. A.; Combrink, K. D.; Gulgeze, H. B.; Venables, B.
31
32 L.; Wright, J. J. K.; Dalterio, R. A.; Zadjura, L.; Marino, A.;
33
34 Dando, S.; D'Arienzo, C.; Kadow, K. F.; Cianci, C. W.; Li, Z.;
35
36 Clarke, J.; Genovesi, E. V.; Medina, I.; Lamb, L.; Colonno, R.
37
38 J.; Yang, Z.; Krystald, M.; Meanwell, N. A. Respiratory
39
40 syncytial virus fusion inhibitors. Part 4: Optimization for oral
41
42 bioavailability. *Bioorg. Med. Chem. Lett.* **2007**, 17, 895-901.
43
44

45
46 23. (a) Mansoor, A.; Mahabadi, N.; Volume of Distribution.
47
48 [Updated 2020 Jul 27]. In: StatPearls [Internet]. Treasure
49
50 Island (FL): StatPearls Publishing; 2020 Jan-. Available from:
51
52 <https://www.ncbi.nlm.nih.gov/books/NBK545280/>. (b) Kazmi, F.;
53
54 Hensley, T.; Pope C.; Funk, R. S.; Loewen, G. J.; Buckley, D.
55
56
57
58
59
60

- 1
2
3 B.; Parkinson, A.. Lysosomal sequestration (trapping) of
4
5 lipophilic amine (cationic amphiphilic drugs) in immortalized
6
7 human hepatocytes. *Drug Metabolism and Disposition*. **2013**, 41,
8
9 897 - 905
10
11
12 24. Branigan, P. J.; Liu, C.; Day, N. D.; Gutshall, L. L.;
13
14 Sarisky, R. T.; Del Vecchio, A. M. Use of a novel cell-based
15
16 fusion reporter assay to explore the host range of human
17
18 respiratory syncytial virus F protein. *Virology Journal*. **2005**,
19
20 2, 54
21
22
23 25. Pickles, R. J. Human airway epithelial cell cultures for
24
25 modeling respiratory syncytial virus infection. *Current Topics*
26
27 *in Microbiology and Immunology*. **2013**, 372, 371-387.
28
29
30 26. Taylor, G. Animal models of respiratory syncytial virus
31
32 infection. *Vaccine* **2017**, 35, 469-480.
33
34
35 27. (a) Böhm, H.-J.; Banner, D.; Bendels, S.; Kansy, M.; Kuhn,
36
37 B.; Müller, K.; Obst-Sander, U.; Stahl, M. Fluorine in medicinal
38
39 chemistry. *ChemBioChem*. **2004**, 5, 637-643. (b) Ghose, A. K.;
40
41 Crippen, G. M. Atomic physicochemical parameters for three-
42
43 dimensional-structure-directed quantitative structure-activity
44
45 relationships. 2. Modeling dispersive and hydrophobic
46
47 interactions. *Journal of Chemical Information and Computing*
48
49 *Science*. **1987**, 27, 21-35.
50
51
52
53 28. Wang, X. A.; Cianci, C. W.; Yu, K. L.; Combrink, K. D.;
54
55 Thuring, J. W.; Zhang, Y.; Civiello, R. L.; Kadow, K. F.; Roach,
56
57
58
59
60

1
2
3 J.; Li, Z.; Langley, D. R.; Krystal, M.; Meanwell, N. A.

4
5 Respiratory syncytial virus fusion inhibitors. Part 5:

6
7 Optimization of benzimidazole substitution patterns towards
8
9 derivatives with improved activity. *Bioorg. Med. Chem. Lett.*

10
11 **2007**, 17, 4592-4598

12
13
14 29. For a discussion of SAR in the Benzimidazolone series see:

15
16 Yu, K-L.; Zhang, Y.; Civiello, R. L.; Trehan, A. K.; Pearce, C.

17
18 P.; Yin, Z.; Combrink, K. D.; Gulgeze, H. B.; Xiangdong, A. W.;

19
20 Kadow, K. F.; Cianci, C. W.; Krystal, M.; Meanwell, N. A.

21
22 Respiratory syncytial inhibitors. Part 2: Benzimidazol-2-one

23
24 derivatives. *Bioorg. Med. Chem. Letts.*, **2004**, 14, 1133 - 1137

25
26
27 30. Kotthaus, J.; Steinmetzer, T.; van de Locht, A.; Clement,

28
29 B. Analysis of highly potent amidine containing inhibitors of

30
31 serine proteases and their N-hydroxylated prodrugs (amidoximes).

32
33 *Journal of Enzyme Inhibition and Medicinal Chemistry*. **2011**, 26,

34
35
36 115-122.

37
38
39 31. Tahri, A.; Vendeville, S. M. H.; Jonckers, T. H. M.;

40
41 Raboisson, P. J.-M. B.; Hu, L.; Demin, S. D.; Coymans, L. P.

42
43 RSV Antiviral Compounds. WO/2014/060411, Apr 24, 2014.

44
45
46 32. Cockerill, G. S.; Hanley, M. T.; Mathews, N.; Paradowski,

47
48 M.; Williams, G.; Ward, S. E. unpublished results.

49
50
51 33. Chapman, J.; Abbott, E.; Alber, D. G.; Baxter, R. C.;

52
53 Bithell, S. K.; Henderson, E. A.; Carter, M. C.; Chambers, P.;

54
55 Chubb, A.; Cockerill, G. S.; Collins, P. L.; Dowdell, V. C.;

1
2
3 Keegan, S. J.; Kelsey, R. D.; Lockyer, M. J.; Luongo, C.;
4
5 Najarro, P.; Pickles, R. J.; Simmonds, M.; Taylor, D.; Tymes, S.;
6
7 Wilson, L. J.; Powell, K. L. RSV604, a novel inhibitor of
8
9 respiratory syncytial virus replication. *Antimicrobial Agents*
10
11 *and Chemotherapy*. **2007**, 51, 3346-3353.

12
13
14 34. Mirabelli, C.; Jaspers, M.; Boon, M.; Jorissen, M.; Koukni,
15
16 M.; Bardiot, D.; Chaltin, P.; Marchand, A.; Neyts, J.; Jochmans,
17
18 D. Differential antiviral activities of respiratory syncytial
19
20 virus (RSV) inhibitors in human airway epithelium. *Journal of*
21
22 *Antimicrobial Chemotherapy*. **2018**, 73, 1823-1829.

23
24
25
26
27
28 35. Morton, C. J.; Cameron, R.; Lawrence, L. J.; Lin, B.; Lowe,
29
30 M.; Luttick, A.; Mason, A.; McKimm-Breschkin, J.; Parker, M. W.;
31
32 Ryan, J.; Smout, M.; Sullivan, J.; Tucker, S. P.; Young, P. R.
33
34 Structural characterization of respiratory syncytial virus
35
36 fusion inhibitor escape mutants: homology model of the F protein
37
38 and a syncytium formation assay. *Virology* **2003**, 311, 275-288.

39
40
41 36. Cianci, C.; Genovesi, E. V.; Lamb, L.; Medina, I.; Yang,
42
43 Z.; Zadjura, L.; Yang, H.; D'Arienzo, C.; Sin, N.; Yu, K. L.;
44
45 Combrink, K.; Li, Z.; Colonno, R.; Meanwell, N.; Clark, J.;
46
47 Krystal, M. Oral efficacy of a respiratory syncytial virus
48
49 inhibitor in rodent models of infection. *Antimicrobial Agents*
50
51 *and Chemotherapy*. **2004**, 48, 2448-54.

- 1
2
3 37. Roymans, D.; Alnajjar, S. S.; Battles, M. B.;
4
5 Sitthicharoenchai, P.; Furmanova-Hollenstein, P.; Rigaux, P.;
6
7 Berg, J. V. D.; Kwanten, L.; Ginderen, M. V.; Verheyen, N.;
8
9 Vranckx, L.; Jaensch, S.; Arnoult, E.; Voorzaat, R.; Gallup, J.
10
11 M.; Larios-Mora, A.; Crabbe, M.; Huntjens, D.; Raboisson, P.;
12
13 Langedijk, J. P.; Ackermann, M. R.; McLellan, J. S.; Vendeville,
14
15 S.; Koul, A. Therapeutic efficacy of a respiratory syncytial
16
17 virus fusion inhibitor. *Nature Communications*. **2017**, 8, 167.
18
19
20
21 38. Battles, M. B.; Langedijk, J. P.; Furmanova-Hollenstein,
22
23 P.; Chaiwatpongsakorn, S.; Costello, H. M.; Kwanten, L.;
24
25 Vranckx, L.; Vink, P.; Jaensch, S.; Jonckers, T. H.; Koul, A.;
26
27 Arnoult, E.; Peeples, M. E.; Roymans, D.; McLellan, J. S.
28
29 Molecular mechanism of respiratory syncytial virus fusion
30
31 inhibitors. *Nat. Chem. Biol.* **2016**, 12, 87-93.
32
33
34
35 39. Cockerill, S.; Mathews, N.; Ward, S.; Lunn, G.; Paradowski,
36
37 M.; Gascon, S. J. M. Spiro-indolines for the treatment and
38
39 prophylaxis of respiratory syncytial virus infection (RSV). WO
40
41 2016/055780, Oct 6, 2016.
42
43
44 40. Cockerill, S.; Pilkington, C.; Lumley, J.; Angell, R.;
45
46 Mathews, N. Pharmaceutical compounds. WO2013/068769, May 16,
47
48 2013.
49
50
51 41. Zhou, M.; En, K.; Hu, Y.; Xu, Y.; Shen, H. C.; Qian, X.
52
53 Zinc triflate-mediated cyclopropanation of oxindoles with vinyl
54
55
56
57
58
59
60

1
2
3 diphenyl sulfonium triflate: a mild reaction with broad
4
5 functional group compatibility. *RSC Advances* **2017**, 7, 3741-3745.

6
7 42. Qin, H.; Miao, Y.; Zhang, K.; Xu, J.; Sun, H.; Liu, W.;
8
9 Feng, F.; Qu, W. A convenient cyclopropanation process of
10
11 oxindoles via bromoethylsulfonium salt. *Tetrahedron* **2018**, 74,
12
13 6809-6814.
14
15

16
17 43. Andreassen, E. J.; Bakke, J. M.; Sletvold, I.; Svensen, H.
18
19 Nucleophilic alkylations of 3-nitropyridines. *Org. Biomol. Chem.*
20
21 **2004**, 2, 2671-2676.
22

23
24 44. Committee for Human Medicinal Products, European Medicines
25
26 Agency. *Guideline on the Clinical Evaluation of Medicinal*
27
28 *Products Indicated for the Prophylaxis or Treatment of*
29
30 *Respiratory Syncytial Virus (RSV) Disease* Draft Guideline,
31
32 EMA/CHMP/257022/2017; London, Oct 30, 2017.

33
34 [https://www.ema.europa.eu/en/documents/scientific-](https://www.ema.europa.eu/en/documents/scientific-guideline/guideline-clinical-evaluation-medicinal-products-indicated-prophylaxis-treatment-respiratory_en.pdf)
35
36 [guideline/guideline-clinical-evaluation-medicinal-products-](https://www.ema.europa.eu/en/documents/scientific-guideline/guideline-clinical-evaluation-medicinal-products-indicated-prophylaxis-treatment-respiratory_en.pdf)
37
38 [indicated-prophylaxis-treatment-respiratory_en.pdf](https://www.ema.europa.eu/en/documents/scientific-guideline/guideline-clinical-evaluation-medicinal-products-indicated-prophylaxis-treatment-respiratory_en.pdf)
39
40

41
42 45. FDA, Center for Drug Evaluation and Research. *Respiratory*
43
44 *Syncytial Virus Infection: Developing Antiviral Drugs for*
45
46 *Prophylaxis and Treatment Guidance for Industry* Draft Guidance,
47
48 Silver Spring, MD; October 2017.

49
50 [https://www.fda.gov/regulatory-information/search-fda-guidance-](https://www.fda.gov/regulatory-information/search-fda-guidance-documents/respiratory-syncytial-virus-infection-developing-antiviral-drugs-prophylaxis-and-treatment-guidance)
51
52 [documents/respiratory-syncytial-virus-infection-developing-](https://www.fda.gov/regulatory-information/search-fda-guidance-documents/respiratory-syncytial-virus-infection-developing-antiviral-drugs-prophylaxis-and-treatment-guidance)
53
54 [antiviral-drugs-prophylaxis-and-treatment-guidance](https://www.fda.gov/regulatory-information/search-fda-guidance-documents/respiratory-syncytial-virus-infection-developing-antiviral-drugs-prophylaxis-and-treatment-guidance)
55
56
57
58
59
60

- 1
2
3 46. DeVincenzo, J. P.; Wilkinson, T.; Vaishnav, A.; Cehelsky,
4 J.; Meyers, R.; Nochur, S.; Harrison, L.; Meeking, P.; Mann, A.;
5 Moane, E.; Oxford, J.; Pareek, R.; Moore, R.; Walsh, E.;
6 Studholme, R.; Dorsett, P.; Alvarez, R.; Lambkin-Williams, R.
7
8 Viral load drives disease in humans experimentally infected with
9
10 respiratory syncytial virus. *American Journal of Respiratory*
11
12 *Critical Care Medicine*. **2010**, 182, 1305-1314.
13
14
15
16
17
18 47. Stevens, M.; Rusch, S.; DeVincenzo, J.; Kim, Y.-I.;
19 Harrison, L.; Meals, E. A.; Boyers, A.; Fok-Seang, J.; Huntjens,
20 D.; Lounis, N.; Mariën, K.; Remmerie, B.; Roymans, D.; Koul, A.;
21 Verloes, R. Antiviral activity of oral JNJ-53718678 in healthy
22 adult volunteers challenged with respiratory syncytial virus: A
23 placebo-controlled study. *The Journal of Infectious Diseases*
24
25 **2018**, 218, 748-756.
26
27
28
29
30
31
32
33
34 48. GileadSciences. Safety Study of GS-5806 to Treat
35 Respiratory Syncytial Virus (RSV). *Clintrials.gov* **2013**,
36
37 NCT01797419. <https://clinicaltrials.gov/ct2/show/NCT01797419>
38
39
40
41
42
43
44 49. (a) Chemaly, R. F.; Dadwal, S. S.; Bergeron, A.; Ljungman,
45 P.; Kim, Y.-J.; Cheng, G.-S.; Pipavath, S. N.; Limaye, A. P.;
46 Blanchard, E.; Winston, D. J.; Stiff, P. J.; Zuckerman, T.;
47 Lachance, S.; Rahav, G.; Small, C. B.; Mullane, K. M.; Patron,
48 R. L.; Lee, D.-G.; Hirsch, H. H.; Waghmare, A.; McKevitt, M.;
49 Jordan, R.; Guo, Y.; German, P.; Porter, D. P.; Gossage, D. L.;

1
2
3 Watkins, T. R.; Marty, F. M.; Chien, J. W.; Boeckh, M. A phase
4
5 2, randomized, double-blind, placebo-controlled trial of
6
7 presatovir for the treatment of respiratory syncytial virus
8
9 upper respiratory tract infection in hematopoietic-cell
10
11 transplant recipients. *Clin. Infect. Dis.* **2019**, 71, 2777-2786.
12
13

14 (b) Marty, F. M.; Chemaly, R. F.; Mullane, K. M.; Lee, D.-G.;
15
16 Hirsch, H. H.; Small, C. B.; Bergeron, A.; Shoham, S.; Ljungman,
17
18 P.; Waghmare, A.; Blanchard, E.; Kim, Y.-J.; McKeivitt, M.;
19
20 Porter, D. P.; Jordan, R.; Guo, Y.; German, P.; Boeckh, M.;
21
22 Watkins, T. R.; Chien, J. W.; Dadwal, S. S. A phase 2b,
23
24 randomized, double-blind, placebo-controlled multicenter study
25
26 evaluating antiviral effects, pharmacokinetics, safety, and
27
28 tolerability of presatovir in hematopoietic cell transplant
29
30 recipients with respiratory syncytial virus (RSV) infection of
31
32 the lower respiratory tract. *Clinical Infectious Diseases.*
33
34
35 **2019**, 71, 2787-2795. .
36
37

38
39 50. Gottlieb J.; Torres F.; Haddad T.; Dhillon G.; Dilling D.
40
41 F.; Knoop C.; Rampolla R.; Walia R.; Ahya V.; Kessler R.; Mason
42
43 D. P.; Budev M.; Neurohr C.; Glanville A. R.; Jordan R.; Porter
44
45 D.; McKeivitt M. T.; German P.; Guo Y.; Chien J. W.; Watkins T.
46
47 R.; Zamora M. A phase 2b, randomized controlled trial of
48
49 presatovir, an oral RSV fusion inhibitor, for the treatment
50
51 of respiratory syncytial virus (RSV) in lung transplant (LT)
52
53 recipients. *J. Heart Lung Transplant.* **2018**, 37, S155.
54
55
56
57
58
59
60

- 1
2
3 51. Hanfelt-Goade, D.; Maimon, N.; Nimer, A.; Riviere, F.;
4
5 Catherinot, E.; Ison, M.; Jeong, S.; Walsh, E.; Gafter-Gvili,
6
7 A.; Nama, S.; Napora, P.; Chowers, M.; Bergeron, A.; Zeltser,
8
9 D.; Moudgil, H.; Limaye, A. P.; Couturaud, F.; Nseir, W.;
10
11 McKevitt, M.; Porter, D.; Jordan, R.; Guo, Y.; German, P.;
12
13 Watkins, T. R.; Gossage, D. L.; Chien, J. W.; Falsey, A. R. A
14
15 Phase 2b, randomized, double-blind, placebo-controlled trial of
16
17 presatovir (GS-5806), a novel oral RSV fusion inhibitor, for the
18
19 treatment of respiratory syncytial virus (RSV) in hospitalized
20
21 adults. *Am. J. Respir. Crit. Care Med.* **2018**, 197, A4457-A4457.
22
23
24
25 52. Brint, M. E.; Hughes, J. M.; Shah, A.; Miller, C. R.;
26
27 Harrison, L. G.; Meals, E. A.; Blanch, J.; Thompson, C. R.;
28
29 Cormier, S. A.; DeVincenzo, J. P. Prolonged viral replication
30
31 and longitudinal viral dynamic differences among respiratory
32
33 syncytial virus infected infants. *Pediatric Researc.* **2017**, 82,
34
35 872-880.
36
37
38
39 53. DeVincenzo, J.; Tait, D.; Efthimiou, J.; Mori, J.; Kim, Y.-
40
41 I.; Thomas, E.; Wilson, L.; Harland, R.; Mathews, N.; Cockerill,
42
43 S.; Powell, K.; Littler, E. A randomized, placebo-controlled,
44
45 respiratory syncytial virus human challenge study of the
46
47 antiviral efficacy, safety, and pharmacokinetics of RV521, an
48
49 inhibitor of the RSV-F protein. *Antimicrob. Agents Chemother.*
50
51 **2020**, 64, e01884-19.
52
53
54
55
56
57
58
59
60

1
2
3
4
5
6
7
8
9
10
11
12
13 Table of Contents Graphic.
14
15
16
17
18
19
20
21
22
23
24
25
26
27
28
29
30
31
32
33
34
35
36
37
38
39
40
41
42
43
44
45
46
47
48
49
50
51
52
53
54
55
56
57
58
59
60

